LANDSLIDE SUSCEPTIBILITY MAPPING: A CASE STUDY OF MALIBAMATŠO SUB-CATCHMENT, LESOTHO.

BY

MATS'ELISO MOCHEKA

201502680

SUPERVISED BY

ASSOC. PROF. BOTLE MAPESHOANE

DISSERTATION SUBMITTED TO THE NATIONAL UNIVERSITY OF LESOTHO WATER INSTITUTE IN PARTIAL FULFILLMENT OF THE REQUIREMENTS FOR THE DEGREE OF MASTERS OF SCIENCE IN INTEGRATED CATCHMENT AND WATER RESOURCES MANAGEMENT

NATIONAL UNIVERSITY OF LESOTHO

OCTOBER 2025

Abstract

Landslide has a serious impact on development and countries' economy. This study presents a geospatial analysis of landslide susceptibility within the Malibamatšo Sub-Catchment, Lesotho, using remote sensing imagery and GIS-based Frequency Ratio (FR) model. The frequency ratio (FR) was used to assess susceptibility to landslides using ten conditioning factors including topography, climate and distance to streams and roads. The conditioning factors datasets were derived from various sources such as DEM, NASA and cadastral maps. The FR weighted thematic layers were then overlaid through numerical addition using the Raster Calculator to generate the Landslide Susceptibility Index (LSI) map which was then classified into 5 categories. Contributing factors of landslide in Malibamatšo Sub-Catchment based on the total frequency ratio (FR) are distance to roads (FR = 15.09), slope aspect (8.79), LULC (5.99) and rainfall (5.09). Areas located within 200 meters of roads exhibited a high landslide susceptibility, with a Frequency Ratio (FR) of up to 4.82. Northeast-facing slopes, areas with bare or agricultural land cover, and regions experiencing high rainfall distribution are generally more susceptible to landslides. Topographic factors such as slope gradient, curvature and elevation are relatively less important, however, Moderate slopes (11–22^{o}) are more prone to landslides than steeper slopes. Soil texture is the least contributing factor (FR = 1.15). The resulting Landslide Susceptibility Map (LSM) classifies the landscape into five susceptibility zones ranging from very low to very high risk. Almost 20% of the catchment is susceptible to the occurrence of landslides. Areas most susceptible to landslides are villages near the national roads and associated with agricultural activities such as Ha Lejone, Ha Taunyane, Ha Sephapo, Taung, Ha Nkisi, and Liphofung. The model's accuracy was validated using the success rate curve (SRC), yielding an Area Under the Curve (AUC) value of 0.89, indicating a high predictive performance. The study's findings support informed decision-making for land use planning, infrastructure development, and the implementation of mitigation strategies in landslide-prone areas.

Key Words: Landslide Susceptibility, GIS, Remote Sensing, Frequency Ratio Model, Contributing Factors.

Declaration

The work contained in this dissertation was carried out and completed by Mats'eliso Mocheka, 201502680 at the National University of Lesotho Water Institute, National University of Lesotho. I hereby declare that this study constitutes my original work and has never been submitted for the award of a degree or diploma to any University. To the best of my knowledge this dissertation contains no material written by another person except where due reference is made in the dissertation itself.

Signature: M.Mocheka **Date:** 07/10/2025

As the candidate's supervisor, I certify the above statement to be correct to my knowledge and have recommended this dissertation for submission.

Assoc. Prof. Name and Surname: Botle Mapeshoane **Date: 07/10/25**

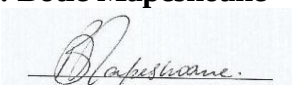

Acknowledgements

I would like to begin by giving all glory and honor to my Lord and Savior, Jesus Christ.

I am profoundly grateful to my supervisor, Associate Professor Botle Mapeshoane, for her unwavering support and guidance throughout the course of this research. Her thoughtful feedback, encouragement, and patience have been invaluable in bringing this dissertation to completion

I would like to thank the following organizations for the role they played in my MSc in ICWRM at the National University of Lesotho.

- The Government of Lesotho in general and the ReNOKA Movement in particular which initiated and coordinated the implementation of the Integrated Catchment Management Programme in Lesotho.
- The EU and German Government for availing the funds for my full scholarship at the NUL.
- Deutsche Gesellschaft für Internationale Zusammenarbeit (GIZ) for providing the necessary technical assistance in the implementation of the ICM Programme under which the MSc in ICWRM Programme was initiated.
- WaterNet for managing the scholarship fund for MSc in ICWRM.
- The National University of Lesotho in general and the Water Institute in particular for running the MSc in ICWRM Programme.

I am sincerely grateful to the Lesotho Meteorological Services (LMS) for providing the data that was vital for my research. I would also like to thank my fellow classmates and friends for their support and collaboration during this journey. Lastly, I am forever indebted to my family for their unconditional love, encouragement, and support throughout my studies.

Contents

List of Tables

List of Figures

Abbreviations and Acronyms

AHP	Analytical Hierarchy Process
AUC	Area Under the Cover
DEM	Digital Elevation Model
FR	Frequency Ratio
GEE	Google Earth Engine
GIS	Geographic Information System
IDW	Inverse Distance Weighting
LCF	Landslide Conditioning Factors
LHDA	Lesotho Highlands Development Authority
LHWP	Lesotho Highlands Water Project
LR	Logical Regression
LSI	Landslide Susceptibility Index
LSM	Landslide Susceptibility Map
LSS	Landslide Susceptibility
LULC	Land Use Land Cover
NDVI	Normalized Difference Vegetation Index
OLI	Operational Land Imager
ROC	Receiver Operating Characteristics
RS	Remote Sensing
SADC	Southern African Development Community
SRC	Success Rate Curve
SRTM	Shuttle Radar Topography Mission
TIRS	Thermal Infrared Sensor
USDA	United States Department of Agriculture
USGS	United States Geological Survey
UTM	Universal Transverse Mercator
WLC	Weighted Linear Combination
WoE	Weight of Evidence

CHAPTER 1: INTRODUCTION

1.1 Background

A landslide is explained as a large volume of soil, rock, or debris sliding down a slope (Zhang et al., 2023). Landslide occurs when the downslope movement influenced by gravity becomes greater than the forces resisting movement, leading to slope failure. It is a geological hazard that is usually connected to extreme occurrences like earthquakes, intense rainstorms, volcanic eruptions, groundwater level fluctuations, snowmelt, stream erosion, human-induced disturbances, or a combination of these factors (Akintan et al., 2023). Landslides happen all around the world, mainly in certain hotspots such as steep terrain, earthquakes, volcanic eruptions, and bare land areas (Makonyo and Zahor, 2023). These areas have conditions that trigger slope instability, leading to frequent landslides. In Africa, landslides happen across most areas, although they are common in the East Africa's high-altitude zones, like, Uganda, Rwanda, Kenya, and Ethiopia. This is due to heavy rainfall, steep slopes, deforestation, and soil erosion, which contribute to slope instability (Makonyo and Zahor, 2023).

Landslides are a contentious problem that has an extensive impact on the socioeconomic systems of the affected communities causing loss of lives, injuries, infrastructure damage, degrade water quality, increase sedimentation, alter land use, displace communities, and threaten biodiversity (Broeckx et al., 2018; Perera et al., 2018). According to Skrzypczak et al. (2017), landslides are environmental processes that result in natural disasters or technological malfunctions, the consequences of which typically endanger people's lives, property, and health.

Landslide is one of the worst natural catastrophes in Africa; nevertheless, few studies have examined the spatial variability of landslide incidents throughout this continent (Broeckx et al., 2018; Igwe, 2018). Globally, landslide susceptibility (LSS) studies indicate that topographical variables are the most important factors controlling landslide occurrences in LSS modelling. Slope gradient is considered a crucial factor in empirical LSS models (Broeckx et al., 2018). In addition to topography, the modelling incorporates other variables such as soil, geology, lithology and land cover classifications, to separate LSS zones within the areas that share similar terrain features (Broeckx et al., 2018). However, variables related to seismic events and precipitation patterns have also been considered critical in assessing landslide susceptibility in Africa. Both seismic activity and precipitation contribute to the weakening of substrates and

reduce stability of the ground through vibrations, weathering, and moisture accumulation resulting in increased susceptibility to landslides causing more severe landslides during subsequent triggers.

Since ancient times, Lesotho has seen a fair number of natural disasters, which have taken different shapes such as floods, drought, heavy snowfall, strong winds, and severe frost (Letsie and Grab, 2015). In recent years, the country has also faced significant geohazard-related challenges, with some areas becoming inaccessible due to landslides, and rock falls, which in turn has led to the flooding of roads and bridges (Adaawen et al., 2023, World Bank Group, 2023). Although landslides were rare in the past in Lesotho, climate change and increasing human activities have led to settlements in high-risk areas, exposing communities to landslides, particularly during heavy rains (The Kingdom of Lesotho Report, 2015). This indicates how crucial mapping landslide susceptibility (LSS) would profit both local communities and policy makers in Lesotho to plan accordingly.

Landslide susceptibility (LSS) is the likelihood that a landslide will happen in a specific place in the future based on historical events under comparable conditions (Tesfa and Sewnet, 2024). Landslide susceptibility mapping (LSM) uses consistent data such as hydrology, geology, and topography, that seldom changes over ten years to examine slope failure proneness (Zhang et al., 2023). Landslide susceptibility mapping is the significant planning, geological hazard risk management and mitigation tool of a region (Dam et al., 2022). Producing landslide susceptibility map is regarded as the initial stage in the preparation, evaluation, and mitigation of landslides (Sonker et al., 2022).

Landslide Susceptibility Map (LSM) can be generated using both qualitative and quantitative methodologies. Qualitative approaches evaluate areas susceptible to landslide by depending on expert knowledge regarding the factors that can start or trigger landslides. The selection and weighting of contributing factors in these methods largely depend on the expertise and practical knowledge and interpretation (Alamrew et al., 2024; Manopkawee and Mankhemthong, 2025). Examples of qualitative methods are Analytical Hierarchy Process (AHP) and Weighted Linear Combination (WLC). Nevertheless, the qualitative approach is often condemned because of its subjectivity in nature, restricted knowledge of the research area, inadequacy of quantitative assessment, and undue assumptions (Arumugam et al., 2023; Manopkawee and Mankhemthong, 2025). Quantitative approaches estimate areas susceptible to landslides by examining the relationship between landslide inventory database and contributing parameters.

Incorporating landslide inventory with contributing factors offers more reliable susceptibility data for landslides. Examples of quantitative methodologies are the weight of evidence model (WoE), Logistic Regression (LR) and Frequency Ratio (FR) model (Das et al., 2023; Manopkawee and Mankhemthong, 2025; Zhang et al., 2023).

Frequency Ratio model has been utilized in several studies to identify the landslide prone areas (Chen et al., 2021; Razavizadeh et al., 2017). Frequency Ratio (FR) model, being a bivariate statistical approach, it functions as a reliable geospatial instrument for determining how independent variables influence the dependent variable probabilistically (Razavizadeh et al., 2017). Frequency Ratio represents the proportion of the area affected by past landslides relative to the total area, along with the ratio of the likelihood of incidence to non-incidence of landslides within a specific attribute (Chen et al., 2021).

1.2 Problem Statement

Although Landslides have been infrequent in Lesotho, their recent occurrence calls for preparedness since they caused significant damage (Kolane, 2022; Lesotho News Agency, 2023; The Kingdom of Lesotho Report, 2015). Several tragic landslides have occurred in the Malibamatšo catchment. These include a case where landslide buried a herder and his livestock alive, highlighting the devastating consequences of landslide (Maseru Metro News, 2021). This natural disaster leads to the loss of human life, in addition to causing severe ecological damage, disrupting human settlements, and adversely affecting local economies (Government of Lesotho Policy, 2011, Segue et al., 2024, The Kingdom of Lesotho Report, 2015).

Similar disasters have been reported elsewhere in the SADC region, where landslides in Zimbabwe's Nyahode and Buzi sub-catchments destroyed infrastructure, displaced communities, and caused significant socio-economic losses (Muchaka et al., 2022). In Malawi and Tanzania, large-scale landslides have resulted in fatalities, severe property damage, and long-term disruptions to local livelihoods, underscoring the urgent need for effective susceptibility assessment and disaster preparedness (Makonyo and Zahor, 2023; Thiery *et al.*, 2024). These growing threats, both within Lesotho and across the wider SADC region, highlight the urgent need for comprehensive landslide susceptibility assessments and mapping efforts to better understand risk patterns and inform effective mitigation and adaptation strategies.

1.3 Justification of the Study

Current reports indicate that Lesotho's geographical and climatic conditions, including its mountainous terrain and susceptibility to severe weather conditions as a result of climate change, are expected to exacerbate the risk of landslides (Adaawen et al., 2023, The Kingdom of Lesotho Report, 2015). It is important to take proactive measures by identifying areas at risk of landslide occurrence and produce susceptibility map (Dam et al., 2022). Such maps enable stakeholders to identify high-risk areas, prioritize monitoring efforts, and guide infrastructure development away from vulnerable zones (Muchaka et al., 2022). Urban planners and infrastructure developers can use these maps to avoid high-risk regions, design safer transportation networks, and plan settlements more resiliently.

Government agencies and emergency response units can apply susceptibility information to strengthen monitoring programmes, early warning systems, and evacuation planning in areas most at risk. Conservation authorities can integrate susceptibility data into watershed management, soil conservation, and land restoration initiatives, while local communities can be educated about landslide hazards, reducing their vulnerability and enhancing resilience.

Moreover, the generation of scientifically grounded susceptibility maps in Lesotho will provide a replicable methodology that can inform policymakers and disaster risk management authorities beyond the national scale. Similar approaches in other Southern African Development Community (SADC) countries such as Zimbabwe, Tanzania, Malawi, and South Africa have proven valuable for regional risk assessment, land-use planning, and infrastructure design (Diko et al., 2014; Makonyo and Zahor, 2023; Muchaka *et al.*, 2022; Thiery *et al.*, 2024). By offering a model for identifying landslide-prone areas across borders, the findings of this study can also support cross-border infrastructure development, promote harmonized disaster risk reduction policies, and strengthen climate resilience strategies across the SADC region.

1.4 Objectives

Research Questions

i) What is the relationship between key conditioning factors (natural and anthropogenic) and landslide occurrence in the Malibamatšo Sub-Catchment?

ii) How reliable is the Frequency Ratio (FR) method in assessing landslide susceptibility in the Malibamatšo Sub-Catchment?

iii) Which areas in Malibamatšo Sub-Catchment are prone to landslide susceptibility on the basis of GIS and remote sensing analysis?

General Objective

The main objective of this study was to map landslide susceptibility utilizing Geographic Information System (GIS), Remote Sensing (RS), and Frequency Ratio (FR) method for the Malibamatšo Sub-Catchment area.

Specific Objectives

i) To evaluate the relationship between conditioning factors and landslide occurrence in the Malibamatšo Sub-Catchment.
ii) To assess the reliability of FR method to assess the susceptibility of the Malibamatšo Sub-Catchment to landslides.
iii) To identify areas within the Malibamatšo Sub-Catchment that are prone to landslides.
iv) To produce a landslide susceptibility map of the Malibamatšo Sub-Catchment

1.5 Hypothesis

There is a significant interrelationship between environmental factors and the occurrence of landslides in the study area. Relative importance of environmental factors influencing landslides occurrence differ between regions.

CHAPTER 2: LITERATURE REVIEW

2.1 Introduction

Landslides carry substantial hazard to both infrastructure and communities, particularly in regions with complex terrain and variable climatic conditions (Ali et al., 2024). LSM seeks to identify regions liable to landslides, which is crucial for minimizing disaster impacts and guiding land-use decisions. It forecasts the regions where future landslides are most probable (Reichenbach *et al.*, 2018).

Methods for LSM fall within three major classifications, namely knowledge-based, physically based, and data-driven approaches. Kknowledge-based approaches are qualitative and the other two are quantitative approaches. Each approach comes with its own strengths and limitations. The knowledge-driven approach, in particular, tends to be more subjective, as it relies heavily on expert understanding of landslide behaviour in a specific area (Chowdhury, 2023). Thus, the importance allocated to each factor is often on the basis of individual opinions and prior experience. Physically based approaches rely on the mechanics of slope failure and the fundamental processes driving landslides and are costly. Data-driven approaches are generally less biased and make use of machine learning and statistical techniques. These methods assign weights on the basis of geo-environmental features of previously occurred landslides, often achieving high accuracy at the regional level while also allowing for relatively quick analysis. Landslide susceptibility mapping is an established global technique for identifying vulnerable regions, however, the use of machine and deep learning algorithms remains quite restricted and there is also very little evidence of physically based methods used to assess landslide susceptibility (Chowdhury, 2023).

Geographic Information Systems (GIS) are broadly applied in landslide susceptibility assessments to integrate spatial data, helping to identify regions with increased hazard potential (Akintan et al., 2023). Geospatial Analysis refers to the practice of examining spatial patterns and relationships within data by utilizing geographic information (like coordinates), remote sensing imagery, and Geographic Information System (GIS) tools to analyze and interpret datasets geographically (M. Viana et al., 2023). GIS and Remote Sensing tools are highly employed and confirmed successful for susceptibility assessment and mapping of landslides (Makonyo and Zahor, 2023). Remote sensing technology is utilized to acquire the data that is subsequently analyzed with GIS, and since it covers large areas both spatially and temporally,

remote sensing is considered a valuable tool (Sonker et al., 2022). GIS tool is primarily used for the analysis of complex data and for interpreting large datasets into more meaningful information (Das et al., 2023). Combining environmental variables such as topography, soil characteristics, and precipitation are essential for predicting landslides and reducing disaster risk (Gulbet and Getahun, 2024). In the context of Lesotho, understanding these factors is critical for disaster management, particularly in the Malibamatšo catchment, which is at risk of landslides as a result of its mountainous terrain (Alamrew et al., 2024).

2.2 Landslide Susceptibility Assessment Using GIS and GIS-Based Models

Scientific evidence has shown the applicability of GIS in assessing landslide susceptibility and understanding environmental factors leading to landslides (Akintan et al., 2023; Alamrew et al., 2024; Ali et al., 2024; Arumugam et al., 2023; Broeckx et al., 2018). For instance, Broeckx et al. (2018) developed "a data-based landslide susceptibility map for Africa", which highlights the role of topography, soil type, and climatic factors in landslide occurrence. Their research emphasized that large-scale, data-driven analyses can reveal key insights into landslide-prone regions, allowing for better disaster management.

In a similar manner, Akintan et al. (2023) conducted a vulnerability study using geotechnical data and GIS in the Okemesi landslide in Nigeria. Their study utilized GIS-based environmental parameters such as lithology, slope, and rainfall to identify locations vulnerable to landslides. The integration of these factors into a spatial model improved the reliability of landslide forecasting, demonstrating the importance of incorporating both geological and environmental data for comprehensive risk assessments.

Ali et al. (2024) conducted a spatial analysis with statistical approaches to assess landslide vulnerability within the Blue Nile Gorge, Ethiopia. Their methodology incorporated multiple statistical techniques to classify risk zones and provided insights into the role of lithology, slope, and hydrological factors. Additionally, Gulbet and Getahum (2024) implemented a combined FR and AHP approach in Awabel Woreda, Ethiopia, revealing that integrating multiple methodologies enhances susceptibility prediction accuracy.

2.3 Landslide Susceptibility Assessment Using GIS and Frequency Ratio (FR) Model

Frequency Ratio (FR) method has been extensively used in landslide risk assessment given its ease of use and reliable performance in quantifying the interaction involving landslide occurrences and conditioning factors (Alamrew et al., 2024; Das et al., 2023). In the northern

part of Los Glaciares National Park, Argentina, Moragues et al. (2024) applied FR model using factors including geomorphology, slope, lithology, aspect, land cover, elevation, curvature, and proximity to geological faults and roads. Their analysis identified land use land cover, geomorphology, and lithology as the most influential factors, with the model achieving an Area Under the Curve (AUC) value of 0.804, indicating good predictive performance.

Similarly, Berhane et al. (2020) conducted a study in the Adwa-Adigrat mountain chains of northern Ethiopia, employing the Frequency Ratio (FR) model using spatial data with multiple classes. Their approach incorporated several influential variables, including slope gradient, LULC, aspect, lithology, and proximity to lineaments and drainage networks. Findings indicated that among the various conditioning factors, lithology, particularly geological units such as tillite, quaternary deposits, reddish sandstone, pyroclasts, Adigrat Sandstone, and associated plugs along with proximity to streams and geological faults as well as slope gradient, were shown to have a notable correlation with landslide incidences, as indicated by their high Frequency Ratio (FR) values. Model's performance was assessed using the Receiver Operating Characteristic (ROC) curve, achieving an Area Under the Curve (AUC) value of 0.70, which indicated moderate but acceptable predictive capability. These findings reinforce the effectiveness of FR model for susceptibility assessment in complex and varied geological terrains.

In northern Thailand's Mae Chan River watershed, Manopkawee and Mankhemthong (2025) utilized FR model to assess landslide susceptibility. Their study incorporated 173 landslide inventory points and nine (9) causative factors, resulting in a susceptibility map where approximately 36% of the area was classified as highly susceptible. Their study identifies landslides as being strongly influenced by the interaction between higher elevated terrain, steeper terrain slope, geology, and land cover with human activities in vulnerable areas also contributing to increased risk. Drainage proximity plays a minor role compared to these other factors. The model's accuracy was validated using AUC values of 0.738 for the success rate and 0.712 for the prediction rate, indicating a reasonably good performance in identifying and predicting landslide-prone areas.

Thapa and Bhandari (2019) focused on the Siwalik Zone in Nepal, integrating multiple thematic layers such as slope, land use, geological structure, drainage proximity, and slope aspect. Their study highlighted how GIS-based preprocessing and classification, followed by the application of Frequency Ratio (FR) model, could effectively delineate landslide-prone

areas. Among the evaluated factors, seasonal heavy rainfall, slope aspect, and proximity to drainage networks were recognized as the most influential contributors to landslide incidence. For model validation, the researchers used both the Success Rate Curve and the Prediction Rate Curve, obtaining Area Under the Curve (AUC) values of 72.55% and 71.73%, respectively. These results demonstrated the model's satisfactory predictive performance and confirmed its adaptability in steep, tectonically active landscapes. The researchers emphasized the FR model's advantage in areas with limited data due to its low computational complexity and straightforward interpretation.

In the context of the Sikkim Himalaya, Sonker et al. (2022) adopted remote sensing and GIS tools alongside the FR method to assess landslide susceptibility. Their analysis demonstrated that distance to roads, NDVI, and land use land cover were major contributing factors, with the generated landslide susceptibility map successfully delineating high-risk areas. The study employed AUC-based validation, confirming the model's robustness in a complex Himalayan environment. The research concluded that FR, when combined with remote sensing data, provides a practical framework for landslide hazard management in mountainous terrain.

Lastly, Pham et al. (2015) conducted a comprehensive FR-based susceptibility assessment "in a section of the Uttarakhand Himalaya, India". Their study utilized spatial datasets covering terrain, land use, and hydrological variables. Specifically, six key variables contributing to landslide occurrence, slope angle, LULC, slope aspect, rainfall elevation, and curvature were considered to evaluate their geographic correlation with landslide occurrences. Model was evaluated using AUC metrics and indicated reliable predictive accuracy. The Area Under the Curve (AUC) for the success rate curve is 0.75, suggesting a reasonably good fit between the Frequency Ratio model and the training data. Meanwhile, the AUC for the prediction rate curve is 0.70, reflecting a satisfactory level of predictive performance by the model. Notably, their findings reinforced the importance of careful factor selection and data preprocessing in ensuring meaningful outcomes. Across all reviewed studies, the use of validation techniques, especially AUC and ROC proved essential in confirming the FR model's predictive quality and ensuring its applicability for landslide risk planning and mitigation in diverse geographical contexts.

In Lesotho, GIS-based models have the potential to inform disaster risk reduction strategies, especially when combined with local data on topography, hydrology, and geology. The use of advanced statistical models, such as those applied by, Berhane et al. (2020), Moragues et al.

(2024), and Sonker et al. (2022), could offer new insights into areas of high vulnerability within the Malibamatšo Catchment, supporting proactive disaster management measures.

2.4 Factors Influencing Landslide Susceptibility

Factors influencing landslide susceptibility include a range of environmental, geological, topographic, and anthropogenic conditions that collectively affect the likelihood and spatial distribution of landslides (Alamrew et al., 2024). For example, in the Mae Chan River watershed of northern Thailand, Manopkawee and Mankhemthong (2025) demonstrated that steeper terrain slope, higher elevated terrain, geology, and land cover significantly intensify likelihood of a landslide initiation. Similarly, Sonker et al. (2025), in their analysis of the Sikkim Himalaya, found that distance to roads, NDVI, and LULC correlated strongly with past landslide events, due to gravitational instability and erosional processes. These findings confirm that slope angle, combined with LULC, Geology and distance to roads is a foundational input in susceptibility modeling, as it directly impacts the balance of forces on a hillslope.

In addition to topography, hydrological and geological factors such as rainfall, drainage proximity, and lithology play key roles in conditioning slope instability. Thapa and Bhandari (2019), working in Nepal's Siwalik Zone, identified seasonal heavy rainfall, slope aspect, and distance to drainage as the greatest influential conditioning factors. Their Frequency Ratio analysis showed that areas closer to drainage lines and those with south- and southeast-facing slopes experienced higher landslide densities, likely due to increased moisture accumulation and solar radiation-induced weathering. Lithological characteristics were also found to influence landslide occurrence in multiple studies. Berhane et al. (2020), for example, emphasized that soft sedimentary rocks such as tillite and reddish sandstone, Adigrat Sandstone, plugs and its associations are more susceptible to failure in the Adwa-Adigrat mountain chains of Ethiopia.

LULC changes are increasingly recognized as human-induced conditioning factors. Deforestation, agricultural expansion, and road construction disrupt the natural equilibrium of slopes. In Los Glaciares National Park, Argentina, Moragues et al. (2025) found that altered land cover and geomorphological units were associated with higher landslide susceptibility. Similarly, Thapa and Bhandari (2019) noted that bare land, anthropogenic land use, such as unplanned settlements and cultivated slopes, exacerbated landslide risk in already vulnerable terrains.

Chen et al. (2021) emphasized the influence of hydrological factors, including precipitation and drainage patterns, in triggering landslides. Their findings align with other studies that identify climatic conditions as critical drivers of landslides, particularly in regions experiencing increased rainfall due to climate change. These studies collectively show that both natural (e.g., geology, hydrology, topography) and human-modified factors must be considered holistically in landslide susceptibility mapping, as they interact in complex ways to influence slope stability.

2.5 Landslide Susceptibility Mapping in the SADC Region

Several recent studies across the Southern African Development Community (SADC) illustrate the application and utility of landslide-susceptibility mapping techniques. In Zimbabwe, Muchaka et al. (2022) applied a combined field- and remote-sensing approach to model landslide susceptibility in the Nyahode and Buzi sub-catchments, demonstrating how inventory-based statistical mapping can identify high-risk zones after severe rainfall events.

In Tanzania, detailed GIS-based susceptibility analyses have been carried out for the Lushoto District, where Makonyo and Zahor (2023) applied spatial modelling techniques to identify and classify landslide-prone areas. Their study demonstrated the effectiveness of GIS-based approaches in integrating topographic, geological, land use, and climatic factors to generate reliable susceptibility maps for planning and disaster risk reduction at the district level.

Recognizing the challenge of selecting appropriate modelling techniques for landslide susceptibility mapping in Tanzania, Muhimbula (2025) investigated methodological performance in Hanang District through a comparative study of three widely used approaches; the Analytical Hierarchy Process (AHP), Frequency Ratio (FR), and Landslide Susceptibility Index (LSI). The results showed that although each model produced broadly similar spatial distributions of high-risk zones, their predictive accuracies differed due to variations in how causative factors were weighted and combined. The ensemble approach, which integrated outputs from all three models, provided the highest predictive performance, indicating that multi-model strategies are more effective in capturing the complexity of slope instability dynamics. This finding underscores the importance of methodological triangulation in susceptibility mapping, especially in data-limited environments where model uncertainty is a significant challenge.

Malawi's progress in this area is particularly noteworthy. Thiery et al. (2024) conducted one of the first national-scale landslide hazard assessments in Africa, integrating landslide inventories with terrain, rainfall, and population data to produce maps that inform disaster risk reduction strategies. Their approach illustrates the power of combining susceptibility modeling with hazard forecasting by including temporal rainfall exceedance probabilities and estimating return periods.

Tchuwa and Makande (2025) conducted an in-depth geotechnical assessment of landslide susceptibility in Blantyre, Malawi, focusing on the surface soils of Soche Hill. The study analyzed five soil profiles (SP.1–SP.5) for key geotechnical parameters, including collapsibility, dispersivity, Atterberg limits, dry unit weight, porosity, and shear strength. The results of this study underscore the critical role of soil properties in landslide susceptibility and highlight the importance of integrating geotechnical data into susceptibility assessments.

In South Africa, research remains limited. However, Diko et al. (2014) analyzed slope instability on selected hills in Limpopo Province, demonstrating the influence of geology, soil properties, and land use on landslide occurrence. These findings underscore the importance of integrating site-specific data with broader spatial models.

2.6 Limitations in Existing Research in the SADC region

Despite significant progress in landslide susceptibility mapping across SADC countries, several limitations are common. Many studies are constrained by incomplete or biased landslide inventories, which limit the robustness and transferability of statistical models (Broeckx et al., 2018). Differences in spatial resolution and scale reduce comparability between local, district, and national-level studies. Ground-truthing and geotechnical field data remain sparse in most SADC research, introducing uncertainties in model outputs (Tchuwa and Makande, 2025). Methodological inconsistencies, including variations in factor selection, weighting, and validation metrics, make cross-country comparisons challenging (Makonyo and Zahor, 2023). Additionally, most susceptibility maps are static and do not incorporate temporal changes such as land-use alteration or climate-induced rainfall shifts, limiting their predictive value for dynamic planning (Thiery et al., 2024). Research in South Africa remains site-specific, and Lesotho currently lacks peer-reviewed scientific studies in this area, highlighting significant regional knowledge gaps and the need for standardized approaches across SADC.

2.7 Disaster Risk Reduction in Lesotho

National Disaster Risk Reduction Policy (The Government of Lesotho, 2011) outlines strategies for mitigating natural hazards, including landslides, through capacity building, public awareness, and infrastructure development. The policy emphasizes the importance of using scientific data and spatial analysis to identify areas at risk of landslides and other environmental hazards.

GIS-based models, as confirmed by Moragues et al. (2024) and Das et al. (2023), offer a valuable tool for implementing these strategies, enabling authorities to prioritize high-risk areas and allocate resources effectively. Despite Lesotho's vulnerability to both soil erosion and landslides, there are no studies specifically focused on the risk of landslides in the country. Broeckx et al. (2018) also noted that many African nations, including Lesotho, lack substantial research on landslides despite their susceptibility. World Bank Group report (2023) indicates that the absence of advanced spatial analysis and predictive tools necessary for accurate forecasting and mitigation of landslides leads to poor disaster management.

However, the interconnection between soil erosion and landslides require further attention. Studies such as Senanayake et al. (2020) and Huang et al. (2020) on soil erosion modeling highlight the need to integrate these two hazards, as areas prone to erosion are also vulnerable to landslides.

2.8 Theoretical Framework

The theoretical foundation of this study is grounded in Ian McHarg's "Design with Nature" (Steiner, 2016), which advocates for planning and design that harmonize with the natural environment. Central to McHarg's approach is the use of overlay mapping to analyze environmental variables, a concept that directly parallels contemporary GIS-based spatial analysis. By layering factors such as slope, soil type, geology, and land use, McHarg demonstrated how to identify areas suitable or unsuitable for development (Cohen, 2019). This theoretical lens is particularly relevant to landslide susceptibility assessment, as it supports the integration of environmental data to inform risk assessment and spatial planning. Building on this foundation, the present study employs geospatial analysis to assess and map areas at risk of landslides, thereby supporting sustainable land-use decision-making in accordance with ecological constraints.

Moreover, Design with Nature theory inherently promotes a proactive rather than reactive approach to managing natural hazards (Daniels, 2019). McHarg's philosophy emphasizes understanding and working within the limits of natural systems, which aligns with anticipating risk through spatial modeling rather than responding after damage has occurred (Bryant and Turner, 2019). In this context, planners and decision-makers are encouraged to develop preventative strategies that respect ecological dynamics. This integration of ecological theory with modern geospatial technology not only reinforces the scientific foundation for hazard mitigation but also supports sustainable development in environmentally sensitive areas.

2.9 Conceptual Framework

According to the studies reviewed and guided by Ian McHarg's Design with Nature theory, this study employs a conceptual framework that integrates geospatial and environmental data for the purpose of landslide susceptibility assessment. As illustrated in Figure 1, the framework begins with a comprehensive data collection and analysis phase, drawing from both primary and secondary sources. Field surveys and interviews provide critical ground-truth data, such as landslide inventory points. Additionally, Google Earth image interpretation supports visual validation and identification of landslide features, enhancing the accuracy of the inventory. Secondary sources include satellite imagery (Landsat, 30m resolution), topographic data (SRTM DEM), and geospatial datasets obtained from the OpenLandMap (USDA System), Lesotho Meteorological Services (LMS), and the Department of Geography at the National University of Lesotho (NUL).

From these sources, key environmental and physical variables are extracted, including land use/land cover, soil texture, rainfall, streams and road networks, and topographic parameters such as slope, aspect, elevation, and curvature. These variables are generally recognized in the literature as causative factors contributing to landslide occurrence. All datasets are imported into ArcGIS, where they undergo preprocessing to ensure consistency in projection, resolution, and spatial extent. This includes resampling to a common cell size (30m x 30m) and reclassification into standardized classes. The output of this stage is a set of thematic maps each representing a single landslide-inducing factor.

Following the generation of thematic layers in ArcGIS, the framework advances into the modeling and analysis phase, where statistical dependencies between landslide occurrences and controlling factors are established. This is achieved through a cross-tabulation process, wherein the geographic distribution of historical landslides is overlaid with each reclassified

factor layer. This step is essential to quantify how strongly each factor correlates with observed landslide events. Frequency Ratio (FR) model is used as the main statistical approach, calculating the likelihood of landslides within every class of the factor based on frequency of landslide incidence relative to area coverage. The computed weights from this method are integrated to create Landslide Susceptibility Index across the area of the study.

End product was a map showing landslide-prone areas (LSM), categorizes the landscape into zones with risk levels ranging from very low to very high susceptibility. This map is a critical instrument for planning and disaster risk managers. To ensure its reliability, the model undergoes validation using the Success Rate Curve (SRC) and the Area Under the Curve (AUC) from ROC analysis, which assess the predictive performance of the model to landslide prone areas. These measures evaluate how effectively the model separates areas at risk of landslides from those that are stable, using landslide inventory for validation. A higher AUC value reflects greater predictive efficiency of the model.

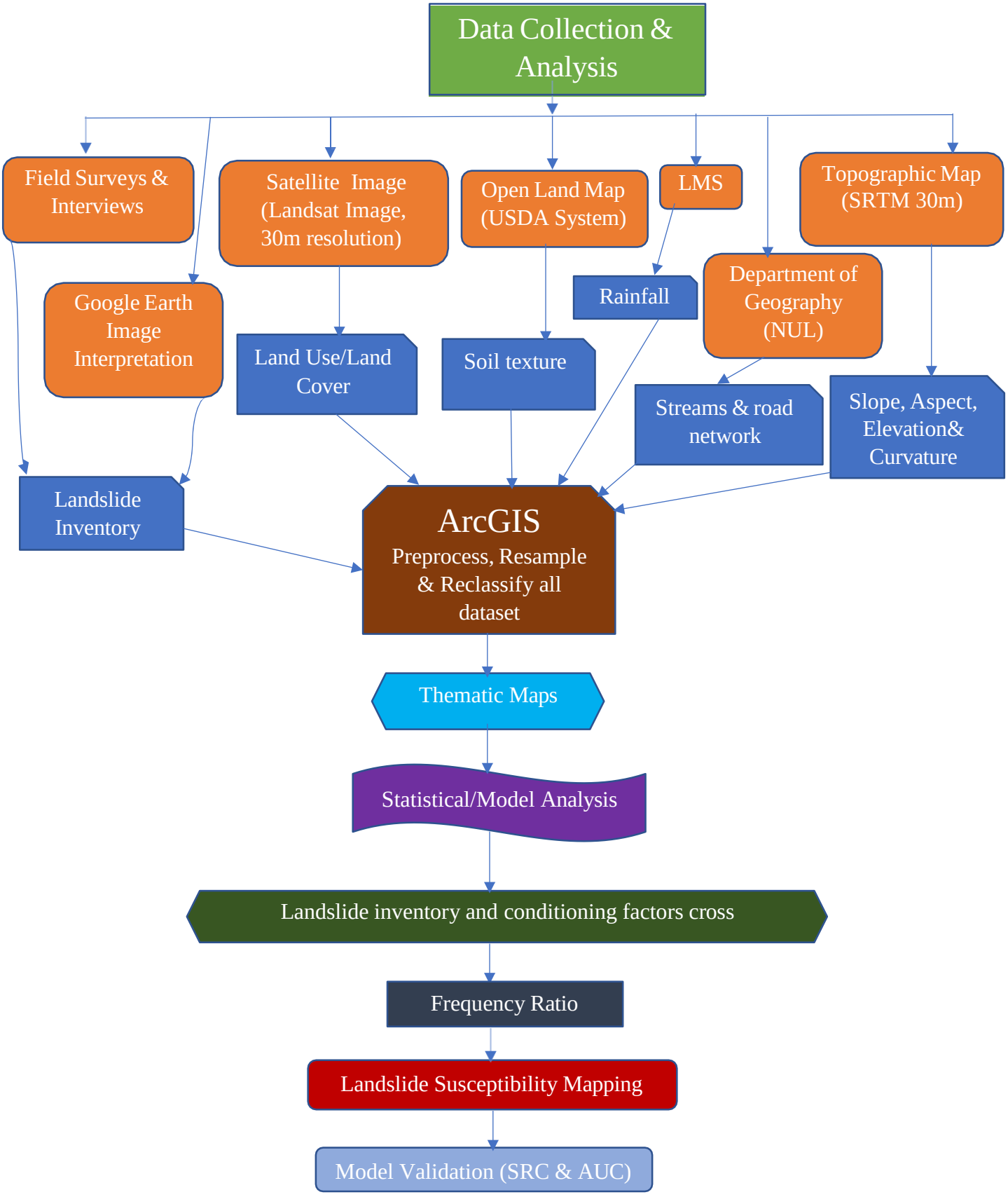

Figure 1. Workflow for the LSM of Malibamatšo Sub-Catchment. The colors in the boxes show the different input data, processes, and results

CHAPTER 3: RESEARCH METHODOLOGY

3.1 Study Area

3.1.1 Location and Climate

Malibamatšo sub-catchment is one of the 74 sub-catchments of Lesotho, located in northern Lesotho in Leribe district (**Error! Reference source not found.**). Lesotho is a mountainous, landlocked country situated entirely within the borders of the Republic of South Africa, positioned on the high plateau of Southern Africa (Khumalo, 2021). The Malibamatšo catchment, covering an area of approximately 318.3 km², lies at altitudes exceeding 2,000 meters above sea level (Mathebula, 2015), with central coordinates around 29.11667°S latitude and 28.48333°E longitude (LHDA, 2017). The river's catchment area is part of Lesotho Highlands Water Project (LHWP) and is impounded by Katse Dam (**Error! Reference source not found.**).

The Malibamatšo River originates near the South African border, draining the Maloti Range's eastern slopes. It flows south past Lejone and joins the Senqu River northeast of Mohlanapeng. The Katse Dam is located in the Malibamatšo Valley, just below is the Bokong River (LHDA, 2017). The Malibamatšo River catchment area's surface water is used for farming, domestic, and livestock purposes. The Liphofung, Mokhoulane and Pelaneng Rivers are tributaries to Malibamatšo River (Mathebula, 2015).

The climate in the Malibamatšo sub-catchment is influenced by its high-altitude location and mountainous terrain (Mathebula, 2015). The mean daily temperature in this area ranges from about 1.96 °C to 12.13 °C. The prevailing wind direction at the site is predominantly westerly, with the highest wind speeds typically occurring in August and the lowest in February. The average wind speed is approximately 5.97 ± 0.07 m/s, measured at a height of 10 m above the ground. This region receives an average annual rainfall of approximately 500–600 mm, with the majority occurring during the summer months between October and March. In addition to rainfall, the region experiences snowfall events each year, although snow contributes less than 10% of the total annual precipitation. Snowfall is particularly common in the winter months, from April to October, when temperatures can fall significantly, reaching lows of around −20 °C (Ntloko et al., 2024).

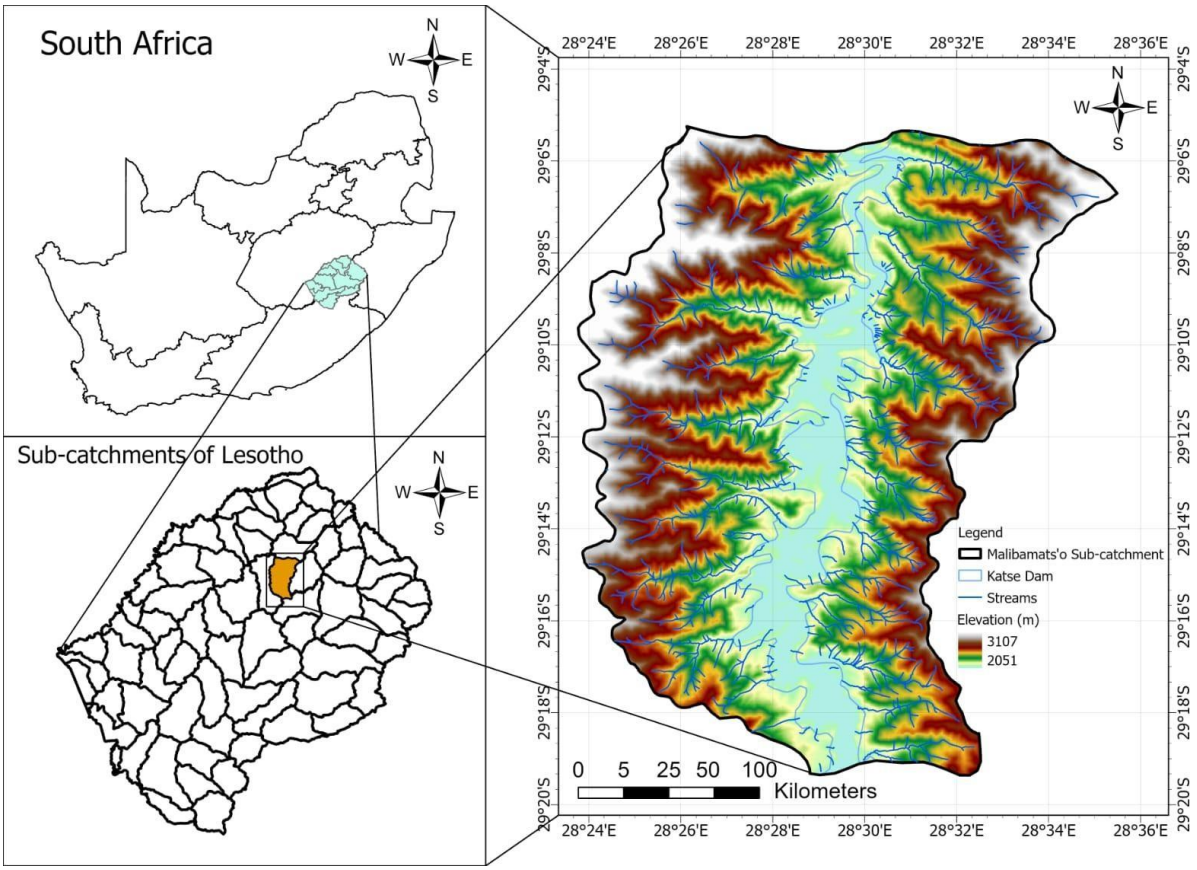

Figure 2: Study Area (Malibamatšo Sub-Catchment)

3.1.2 Geology and Soils of Malibamatšo Sub-Catchment

The study area lies within the Maloti (Maloti–Drakensberg) highlands and is underlain predominantly by flood basalts of the Drakensberg Group often referred to locally as the Lesotho Formation, Jurassic-age (183 Ma) tholeiitic basalt flow sequences that form the high plateau and escarpment morphology of Lesotho (Greyling and Hedding, 2025). These basalt flows form extensive, flat-lying to gently dipping sheet flows, commonly show columnar jointing and amygdaloidal horizons, and rest above underlying Clarens/Stormberg siliciclastic units where exposed in valley cuts (Ntloko *et al.*, 2024). The Drakensberg basalts control regional relief, drainage patterns and cliffed escarpments that are important for slope stability and geomorphic processes in the Maloti region (Fitchett and Mackay, 2025).

Soils developed on the Drakensberg (basalt) terrain are generally shallow, lithic/lithosolic in character and often clay-rich in the fine fraction where weathering is advanced. Where drainage permits (wetlands, valley floors) soils show higher silt/clay content, greater organic carbon and elevated base cation concentrations; on steeper slopes and plateau surfaces soils are thin, poorly developed (apedal/lithic profiles) and prone to erosion (Fitchett and Mackay, 2025). The soils

in this area can be classified into four main groups: shallow sandy loam soils; moderately deep to deep sandy loam soils; clayey soils with very low organic matter content; and soils composed primarily of partially weathered rock fragments (Ntloko et al., 2024).

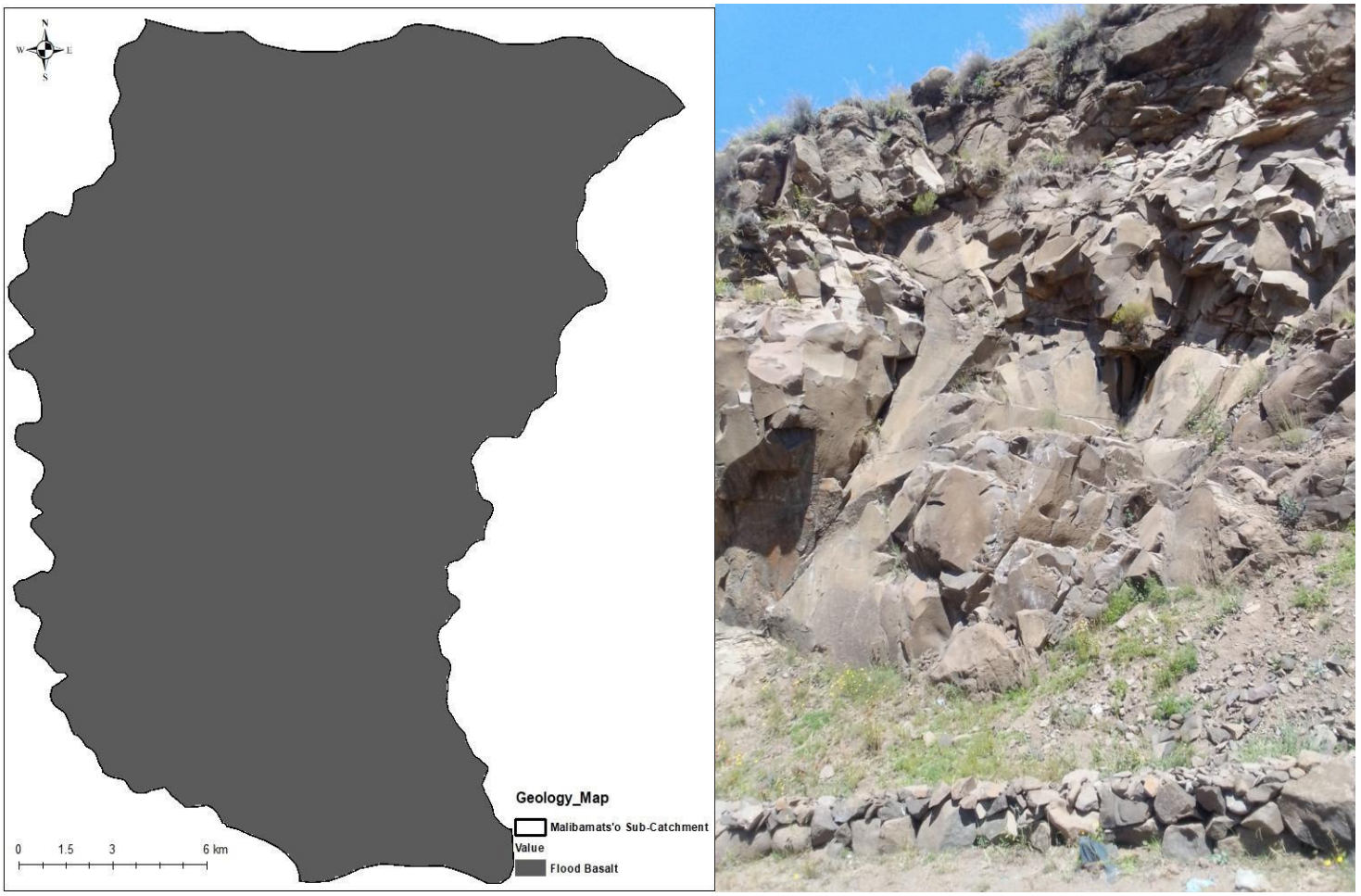

Figure 3: Geology of Malibamatso Sub-Catchment

3.2 Methods of Data Collection

The study employed a combination of primary and secondary datasets. Methods of data collection for Primary datasets involved interviews and physical field observations, while secondary data involved the remotely sensed data on physical land features relevant in landslides occurrences.

3.2.1 Primary Data

Primary data were derived from interviews and field observation. Three field visits were performed to obtain data needed for the study. The first phase of field visits involved conducting interviews with local residents and authorities in order to acquire information on the history and characteristics of past landslides. The second phase field visit focused on collecting geospatial data from landslide sites using GPS to accurately record their locations. Geo-referenced field observations were as historical landslides areas, which served as a base map or landslide inventory map.

Interviews were conducted using semi-structured formats and administered through a digital questionnaire designed and deployed via KoboToolbox. The KoboCollect mobile application was used to conduct the interviews in the field, allowing for real-time data entry and secure storage. The questionnaire included both closed and open-ended questions, focusing on local perceptions of landslide triggers, affected areas, and community responses. Interviewees were purposively selected based on their local knowledge and experience with landslides, including residents of high-risk areas, and local leaders.

3.2.2 Secondary Data

Secondary datasets collected include topographic, vegetation, climatic and soil variables. 30m resolution Shuttle Radar Topography Mission (SRTM) Digital Elevation Model (DEM) dataset was acquired from the United States Geological Survey (USGS) to prepare elevation, slope aspect, slope curvature, and slope angle layers. Landsat images with a resolution of 30m, that is Landsat 8-9 OLI/TIRS C2 L1 Images from 2010-2020 were used to prepare Land Use Land Cover and NDVI maps. Soil texture data were sourced from the United States Department of Agriculture (USDA) soil database through the Google Earth Engine (GEE) platform. Rainfall data were obtained from the Lesotho Meteorological Services. This included 11 years of daily rainfall records from 2010 to 2020, collected from two nearby rainfall stations selected for the

study. Streams and Road networks data were obtained from cadastral maps developed by Department of Geography National University of Lesotho.

Table 1. Data sets of the Study

Datasets	Parameters	Source	Scale or resolution	Classification method
Shuttle Radar Topography Mission (SRTM) DEM	Slope	USGS Earth Explorer	30m x 30m	Natural break
	Elevation		30m x 30m	Natural break
	Aspect		30m x 30m	Natural break
	Curvature		30m x 30m	Natural break
Road network data	Road Distance	Department of Geography NUL	30m x 30m	Natural break
Streams network data	Stream Distance		30m x 30m	Natural break
Rainfall data	Rainfall	Lesotho Meteorological Service (LMS)	30m x 30m	Natural break
Soil texture data	Soil Texture	Google Earth Engine (GEE) USDA	30m x 30m	Natural break
Landsat 8-9 OLI/TIRS	LULC	USGS Earth Explorer	30m x 30m	Unsupervised classification
	NDVI		30m x 30m	Unsupervised classification

3.3 Data Analysis

All the datasets were processed using ArcGIS 10.8. Data were harmonized to similar projection and resolution. All data were projected to WGS 1984 Universal Transverse Mercator (UTM) Zone 35S and spatial resolution of 30 m. Thereafter, layers were classified using the Jenks natural breaks method within the ArcGIS application. This approach helps in identifying meaningful groupings and patterns without any bias (Fuad et al., 2024). Landslide Inventory Map served as the base map, providing the reference layer for identifying historical landslide locations. Together, these factor maps and the base map were integrated to create the final landslide susceptibility map for the area of study.

3.3.1 Landslide Conditioning Factors (LCF)

In this study, ten (10) influencing parameters were carefully selected, considering existing literature, their effectiveness, data availability, and relevance to landslide occurrence. These conditioning factors include elevation, aspect, slope gradient, curvature, soil texture, distance to roads and streams, rainfall, normalized differential vegetation index (NDVI) and land use land cover. Digital Elevation Model (DEM) data were utilized in ArcMap 10.8 to generate key topographic parameters of the Malibamatšo sub-catchment, such as elevation, aspect, slope gradient, and slope curvature with the help of the Spatial Analyst tool under the Surface function.

Land use Land cover map was derived from Landsat 8-9 satellite imagery using unsupervised classification technique in ArcMap 10.8, categorizing it into seven classes. The Normalized Difference Vegetation Index (NDVI) is a standardized measure of greenness (relative biomass) and vegetation density over space. In this study, NDVI was derived from Landsat 8-9, using Near-Infrared and Red bands within ArcGIS environment. The resulting NDVI raster was reclassified to highlight areas with varying levels of vegetation cover, from bare soil to dense vegetation. NDVI values were derived using the following equation:

$$NDVI = (IR - R)/ (IR + R)$$

Where IR = Near-Infra Red band

R = Red band

In the study area, NDVI ranges from −0.058 to 0.517.

For this study, rainfall map was created from daily rainfall data from Lesotho Meteorological Services. To create rainfall pattern map, daily rainfall data was processed in Microsoft Excel, including data cleaning and formatting. Monthly totals were calculated, and the mean annual rainfall was derived for each station by averaging over the study period. The data was then imported into ArcGIS 10.8, georeferenced using station coordinates, and converted to a point Shapefile. In the final stage, the Inverse Distance Weighting (IDW) technique was employed to generate spatial rainfall distribution map.

The mixture of sand, silt, and clay particles, referred to as soil texture, also has impact on soil stability, moisture retention, and drainage efficiency. These properties affect the shear strength and susceptibility of soil to erosion, making texture a critical factor in landslide occurrence.

Soil texture data was extracted from Google Earth Engine (GEE) using the USDA SoilGrids dataset, clipped to the study area, and exported as a GeoTIFF. The data was imported into ArcGIS, projected for spatial accuracy, and classified into three textural classes.

Stream distance analysis was conducted using secondary data of the stream network. The stream network Shapefile was imported into ArcGIS, and the Multiple Ring Buffer tool was applied to create distance buffers around the streams at intervals. The buffers were then merged to create a single distance layer, symbolized to show zones of varying proximity to streams. Likewise, road distance was analyzed using Multiple Ring Buffer in ArcGIS based on secondary road network data. The road network Shapefile was imported, and multiple buffer areas were established at specified distances to capture the varying impact of roads. The Multiple Ring Buffer tool was employed to create concentric distance layers around the roads.

3.3.1 Landslide Inventory Mapping

The landslide inventory map illustrates the spatial distribution of historical landslides across different regions, providing insights into the geographic patterns of landslide occurrences (Segue et al., 2024). Figure 4 shows landslides that occurred in the sub-catchment in 2019 and 2021.

Figure 4: Historical Landslide between ha Poli and ha Thibeli (on the left) and Pitseng (on the right) in Malibamatšo Sub-Catchment

(Source: https://x.com/TheReporterLS/status/1482738681400147973)

A total of 13 landslides were identified and documented by the researcher during the course of this study (Figure 5). Their identification relied on combined remote sensing data techniques and field investigations. Ground surveys were carried out to confirm and enhance the remotely obtained data. Additionally, landslides were visually interpreted and digitized using Google Earth's high-resolution imagery to further update the landslide inventory remotely. Each landslide was delineated as a polygon feature using a combination of field mapping and desktop analysis. Field observations and GPS data were employed to verify and refine the landslide boundaries. These boundaries were digitized in Google Earth Pro as part of the GIS mapping process and subsequently imported into ArcGIS for further spatial analysis. For more detailed examination, the polygon features were transformed into raster format using a spatial resolution of 30 meters by 30 meters and projected using the WGS 1984 UTM Zone 35S coordinate system. The resulting polygons formed the landslide inventory map. The recorded events included three main types of landslides: debris flows, debris slides, and rockfall.

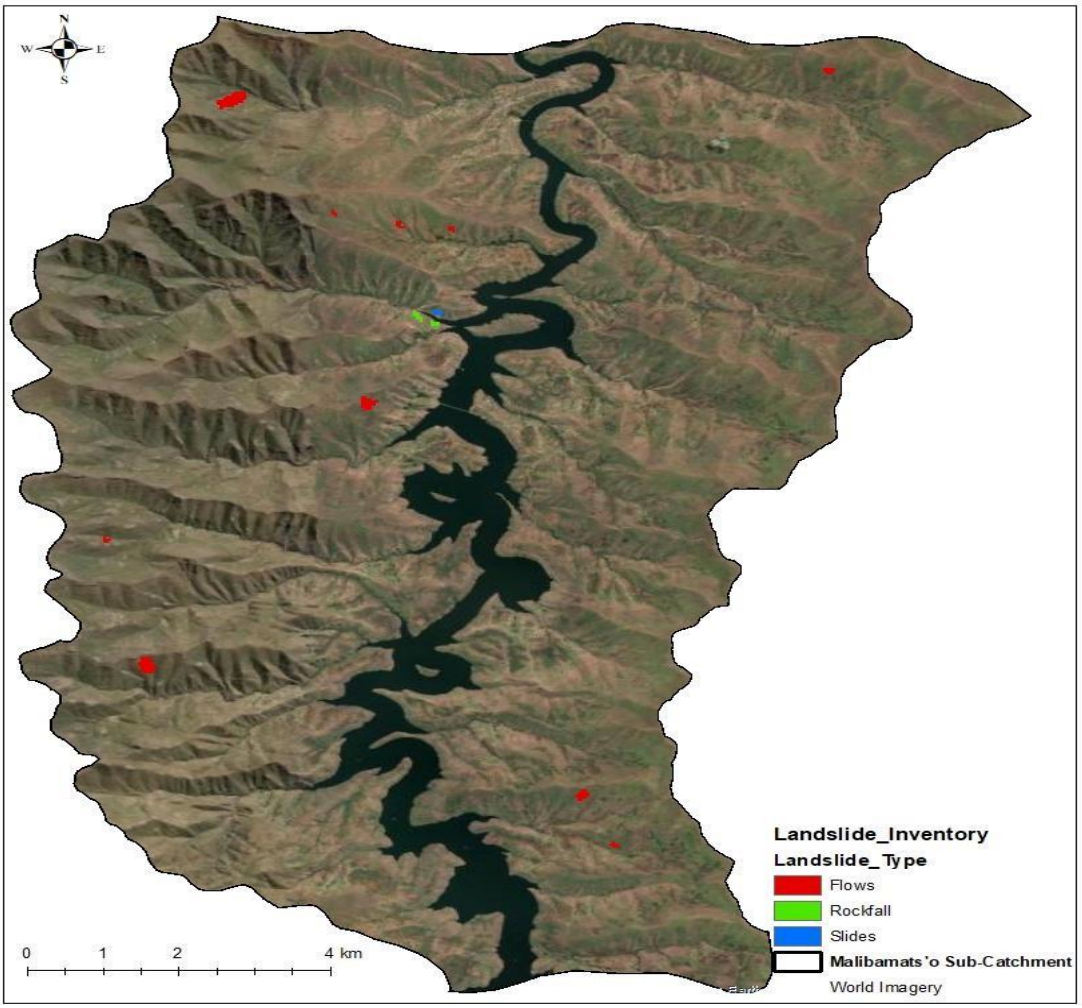

Figure 5: Landslide Inventory Map

3.3.2 Community Perceptions

The data collected through KoboToolbox were exported into Microsoft Excel for analysis. Closed-ended responses were analyzed quantitatively by employing descriptive statistics specifically frequency counts and percentages. Open-ended responses were analyzed using thematic analysis, where qualitative answers were reviewed, coded, and grouped into common themes. Recurring themes included the observation that landslides are frequently provoked by intense rainfall and are often connected with exposed land lacking vegetation cover, especially in cultivated areas and grazing land. These themes were identified manually to draw insights from the local knowledge provided by interviewees.

According to the interviewees, landslides in their area are predominantly triggered by the presence of exposed land lacking vegetation cover. They noted that heavy and intense rainfall events often initiate these landslides, particularly on agricultural fields.

3.4 Statistical Analysis

Using the base map and the thematic factor maps, a landslide susceptibility map was generated. In the present study, Frequency Ratio (FR) method was employed to quantitatively assess the area's landslide susceptibility. This was accomplished by assessing spatial relationship between past landslide events and the contributing environmental factors. To assess how each factor contributes to landslide susceptibility, the landslide inventory was individually overlaid with each thematic data layer. The frequency ratio for each class within a factor was then computed using a three-step process. Firstly, using ArcGIS 10.8, the area where landslides occurred and did not occur was measured for each class. Secondly, still in the ArcGIS environment, the proportion of each class relative to the total area of the factor was determined. Thirdly, FR values for all the conditioning factor maps used in this study were calculated using ArcGIS 10.8 and Microsoft Excel. To do this, the reclassified cell values from each factor map were copied from attribute table in ArcGIS into Excel Software and labeled as factor classes. The corresponding number of landslide pixels for each class was also recorded. Finally, the FR for each class was computed by dividing the percentage of landslide pixels in that class by the percentage of the total area represented by the same class.

Equation (1)

$$FR = \frac{\%\ of\ landslide\ pixels}{\%\ \text{of the total class pixels}}$$

The Frequency Ratio (FR) values obtained were used as weights and assigned to the corresponding classes in each factor map, resulting in weighted thematic layers. These weighted maps were then overlaid through numerical addition using the Raster Calculator to generate the Landslide Susceptibility Index (LSI) map.

Equation (2)

$$LSI = \sum_{i=1}^{n} \text{FR}i$$

Where:

N = Total number of contributing factors.

FRi = Frequency ratio of the i-th factor class.

The calculated FR values for each pixel in the LSI map represent the relative likelihood of landslide incidence. Pixels exhibiting higher LSI values signify areas with greater landslide risk, while areas displaying lower values reflect a lower degree of susceptibility. Different methods can be employed to classify landslide susceptibility index values, namely equal interval, natural breaks, and standard deviation approaches (Thapa and Bhandari, 2019b). Among these, the natural breaks method is the most commonly applied and was therefore chosen for this study. Applying this method, the landslide susceptibility index was categorized into five classes: (1) Very Low, (2) Low, (3) Moderate, (4) High, and (5) Very High.

3.5 Validation

Map validation serves as the last stage in the evaluation of landslide susceptibility, confirming the accuracy of the anticipated outcomes (Thapa and Bhandari, 2019). In the current study, the credibility of the landslide susceptibility map was validated using success rate to verify the reliability of the predictive outcomes. The success rate curve was generated through the visualization of the cumulative percentage of known landslide occurrences against the cumulative percentage of the area classified in the susceptibility map. To generate the success rate curve for LSI map, all pixel index values were first sorted in descending order. The sorted values were then divided into 17 classes, each representing a 1% cumulative interval. The classified map was overlaid with the landslide inventory map, and a cross-tabulation was performed. The resulting values from the cross table were used to construct the success rate curve. The reliability of the Frequency Ratio model was then evaluated using the Area Under the Curve (AUC) method. The AUC was computed using the trapezoidal rule.

Equation (3)

$$AUC = \sum[(\mathrm{Xi} + 1 - \mathrm{Xi}) * (\frac{Yi + 1 + Yi}{2})]$$

Where:

- Xi = Cumulative percentage of study area
- Yi = Cumulative percentage of landslides

The relationship between AUC values and prediction accuracy, both quantitatively and qualitatively, can be categorized as follows: an AUC of 0.5–0.6 indicates poor accuracy, 0.6–0.7 reflects an average level, 0.7–0.8 is considered good, 0.8–0.9 is deemed very good, and values between 0.9–1.0 represent excellent prediction accuracy (Gulbet and Getahun, 2024b).

3.6 Methodological Limitations of the Study

The Frequency Ratio (FR) model combined with GIS offers a practical approach for landslide susceptibility mapping, but several limitations were encountered in this study. A notable limitation encountered in this study was related to the application of the Frequency Ratio (FR) model to parameters with no variability. For instance, the geological factor in the study area was dominated entirely by a single lithology, namely flood basalt. Since the FR model requires at least two classes within a parameter to calculate frequency ratios, it was not possible to include geology as a contributing factor in the analysis. This limitation highlights the dependency of FR on the presence of categorical variability in the input datasets.

Additionally, the FR model assumes independence between causative factors, which may not reflect real-world interactions where factors such as slope, aspect, and land cover are often interrelated. The model is also sensitive to data quality and resolution, meaning that coarse-resolution DEMs or incomplete datasets, such as missing rainfall or road distance data can reduce the accuracy of the analysis. Furthermore, FR is a bivariate statistical approach, considering each factor separately, and does not account for dynamic temporal changes such as vegetation growth, land use modifications, or climatic variability. Finally, the model provides probabilistic susceptibility maps but cannot predict the precise timing or magnitude of future landslides. These limitations highlight the need for careful data preparation and, where possible, the integration of more advanced or multivariate modeling approaches for improved predictive accuracy.

CHAPTER 4. RESULTS AND DISCUSSION

4.1. Factors that are important in LSS in the Malibamatšo Sub-Catchment

Frequency ratio (FR) represents the proportion of landslide occurrences within a specific class relative to the total area of that class. A value of 1 indicates an average level of susceptibility, meaning landslides occur in that class at a rate proportional to its area. Values greater than 1 suggest higher susceptibility, while values less than 1 indicate lower susceptibility (Moragues et al., 2024 p.10).

Table 2: Frequency Ratio Value Calculations for Curvature

Parameter	Classes	Class Pixels	% Class Pixels (a)	Landslide Pixels	% Landslide Pixels (b)	FR (b/a)
Curvature	Concave	102541	28.64	79	32.92	**1.15**
	Flat	135652	37.89	101	42.08	**1.11**
	Convex	119851	33.47	60	25.00	0.75
Total		358044	100	240	100	**3.01**

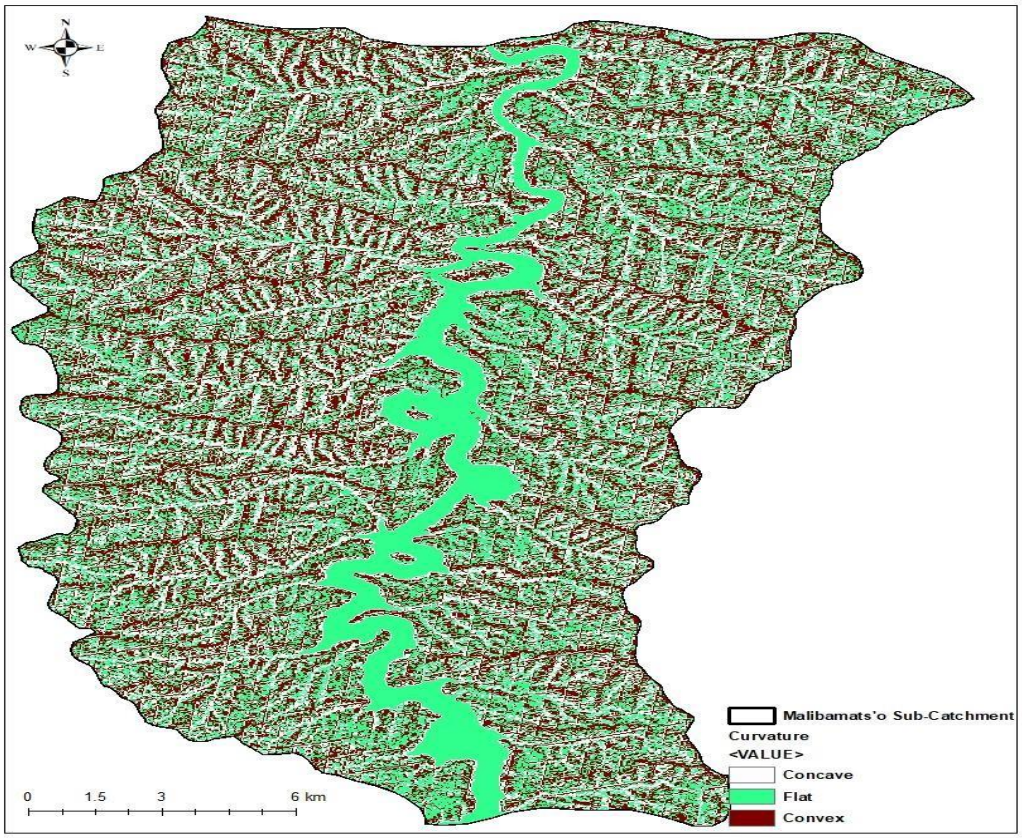

Figure 6: Curvature Map

Table 3: Frequency Ratio Value Calculations for Slope Angle

Parameter	Classes	Class Pixels	% Class Pixels (a)	Landslide Pixels	% Landslide Pixels (b)	FR (b/a)
Slope angle (degree)	0 - 11	78879	22.19	10	4.17	0.19
	11 - 22	148267	41.71	162	67.50	**1.62**
	22 - 33	117385	33.02	59	24.58	0.74
	33 - 45	10700	3.01	9	3.75	**1.25**
	>45	215	0.06	0	0.00	0.00
Total		355446	100	240	100	**3.80**

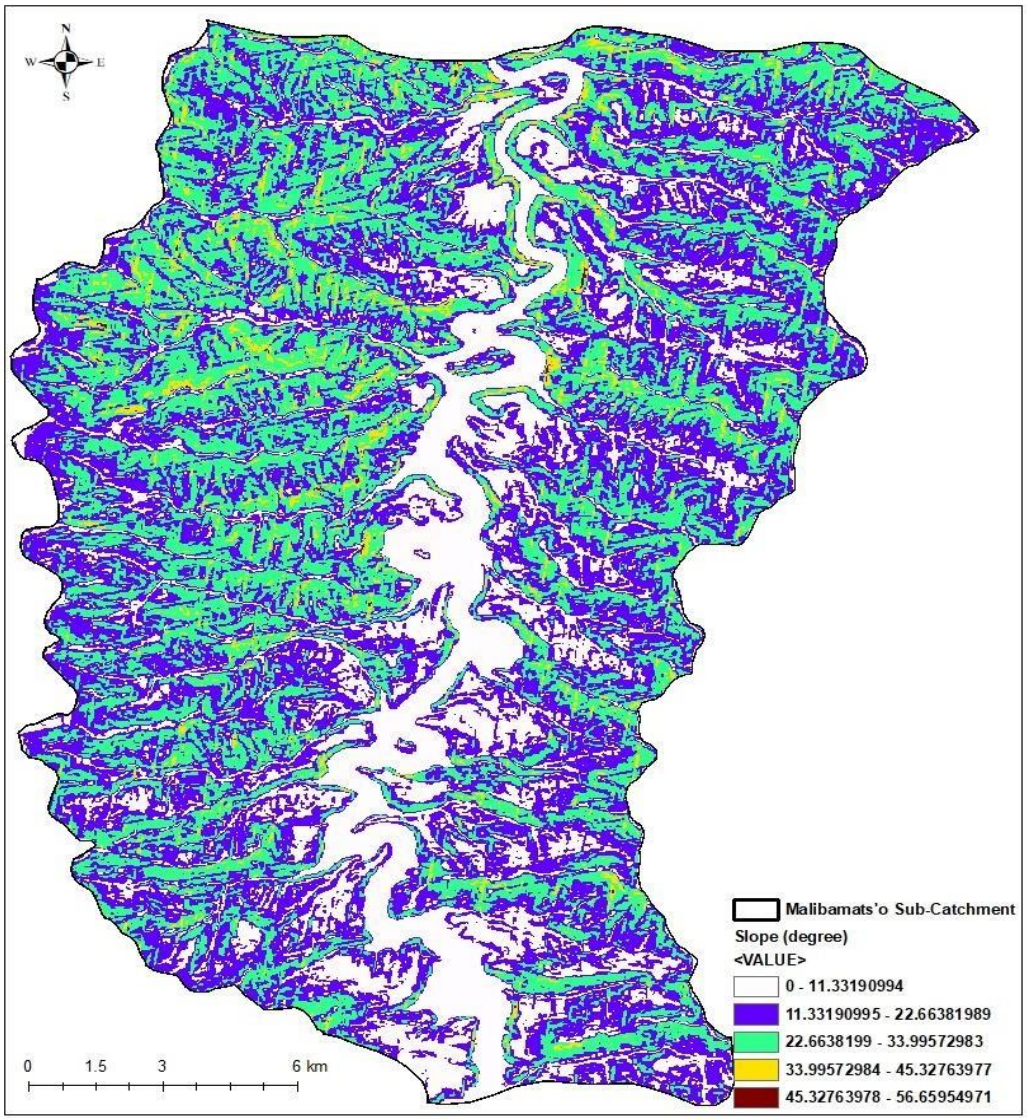

Figure 7: Slope Angle Map

Table 4: Frequency Ratio Value Calculations for Elevation

Parameter	Classes	Class Pixels	% Class Pixels (a)	Landslide Pixels	% Landslide Pixels (b)	FR (b/a)
Elevation (m)	2051 -2262	119880	33.48	60	25.00	0.75
	2262 - 2473	98370	27.47	7	2.92	0.11
	2473 - 2684	82985	23.18	145	60.42	**2.61**
	2684 - 2895	44930	12.55	28	11.67	0.93
	2895 - 3107	11879	3.32	0	0.00	0.00
Total		358044	100	240	100	**4.39**

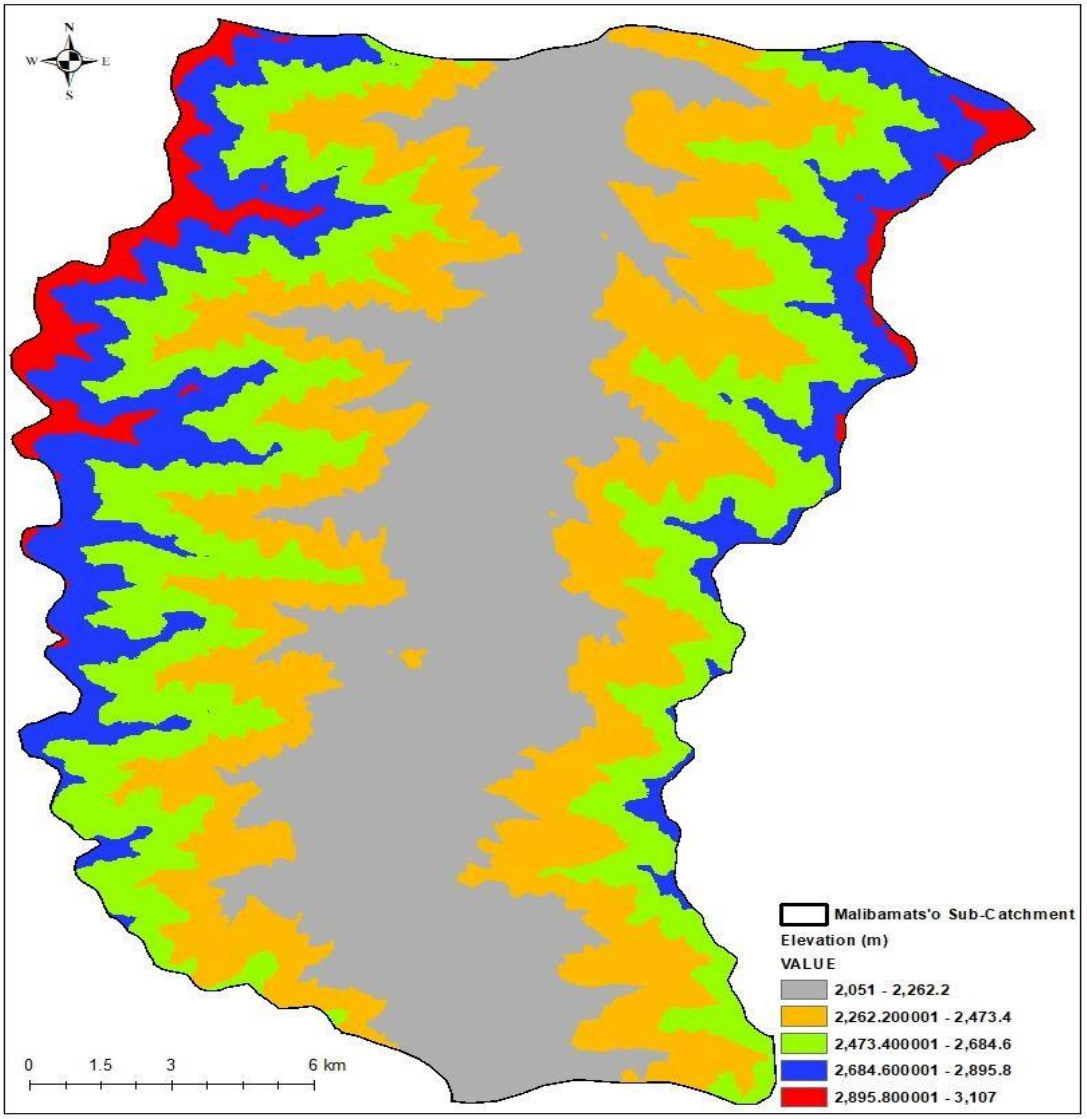

Figure 8: Elevation Map

Table 5: Frequency Ratio Value Calculation for Slope Aspect

Parameter	Classes	Class Pixels	% Class Pixels (a)	Landslide Pixels	% Landslide Pixels (b)	FR (b/a)
Slope Aspect (degree)	Flat – N (-1 - 40)	65056	18.30	45	18.75	**1.02**
	NE (40 – 80)	40085	11.28	143	59.58	**5.28**
	E (80 – 120)	28984	8.15	39	16.25	**1.99**
	SE (120 – 160)	36014	10.13	1	0.42	0.04
	S (160 – 200)	39495	11.11	7	2.92	0.26
	SW(200 – 240)	39255	11.04	5	2.08	0.19
	W (240 – 280)	32493	9.14	0	0.00	0.00
	NW (280 – 320)	31392	8.83	0	0.00	0.00
	N (320 – 360)	42672	12.01	0	0.00	0.00
Total		355446	100	240	100	**8.79**

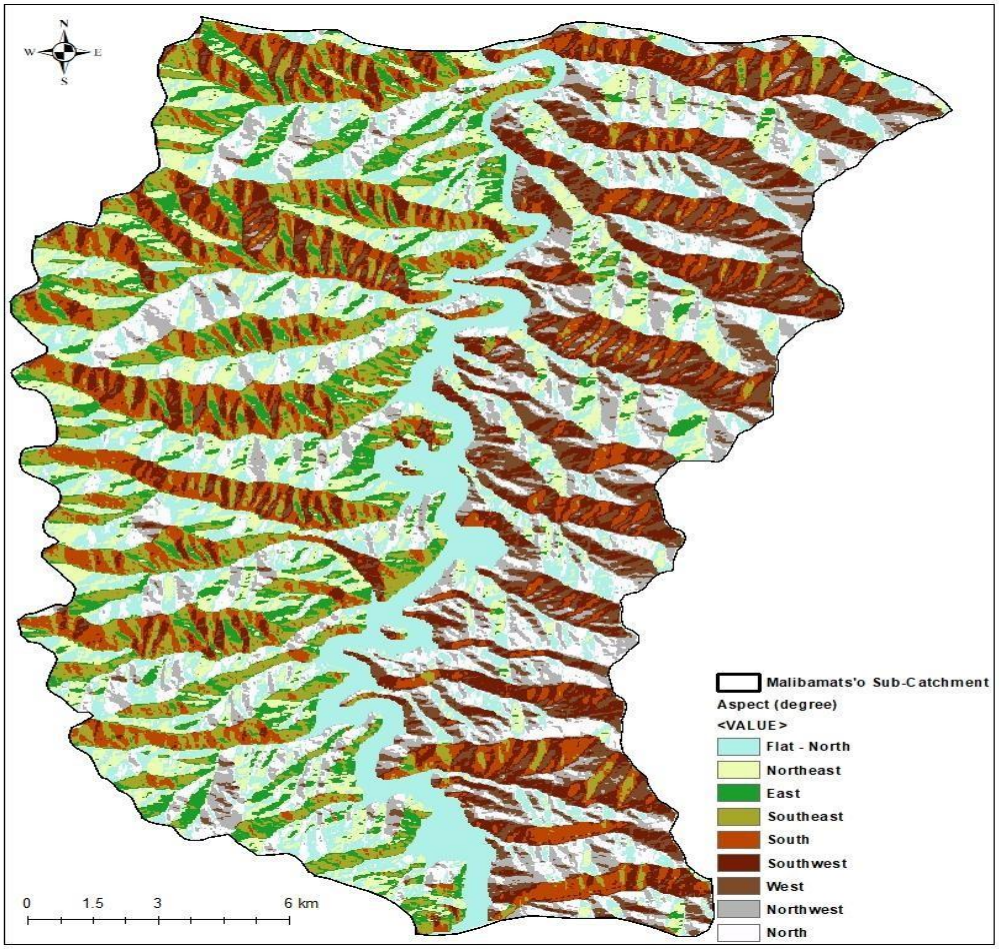

Figure 9: Slope Aspect Map

Table 6: Frequency Ratio Value Calculations for LULC

Parameter	Classes	Class Pixels	% Class Pixels (a)	Landslide Pixels	% Landslide Pixels (b)	FR (b/a_
LULC	Water Body	23251	6.49	0	0.00	0.00
	Grassland	47930	13.39	2	0.83	0.06
	Shrubs	50057	13.98	11	4.58	0.33
	Bareland	65430	18.27	97	40.42	**2.21**
	Sparse Vegetation	67223	18.77	43	17.92	0.95
	Buildup Area	50736	14.17	5	2.08	0.15
	Agricultural Land	53420	14.92	82	34.17	**2.29**
Total		358047	100	240	100	**5.99**

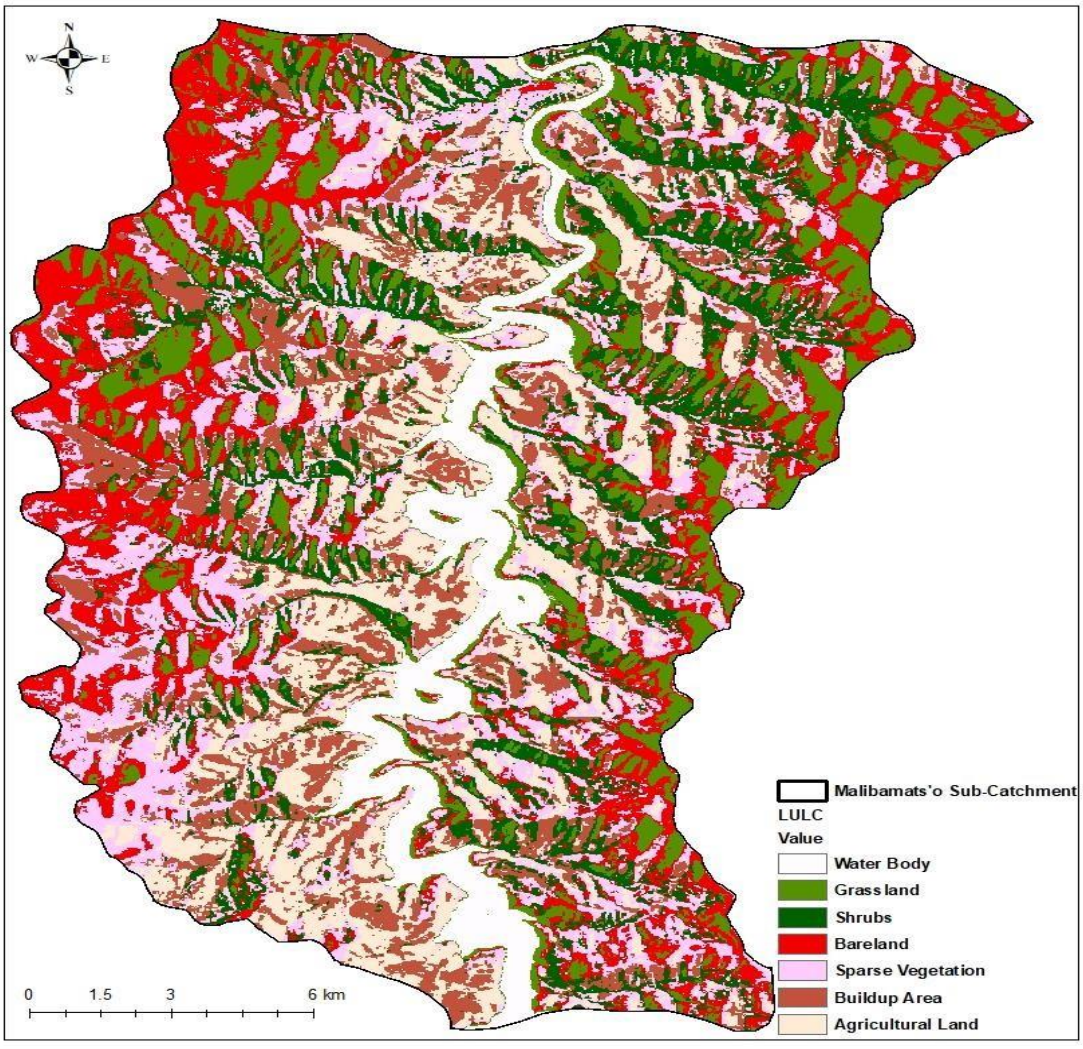

Figure 10: Land Use Land Cover Map

Table 7: Frequency Ratio Value Calculations for Soil Texture

Parameter	Classes	Class Pixels	% Class Pixels (a)	Landslide Pixels	% Landslide Pixels (b)	FR (b/a)
Soil Texture Classes	Water	35568	9.93	0	0.00	0.00
	Sandy Clay Loam	11960	3.34	0	0.00	0.00
	Loam	310338	86.64	240	100.00	**1.15**
	Sandy Loam	320	0.09	0	0.00	0.00
Total		358186	100	240	100	**1.15**

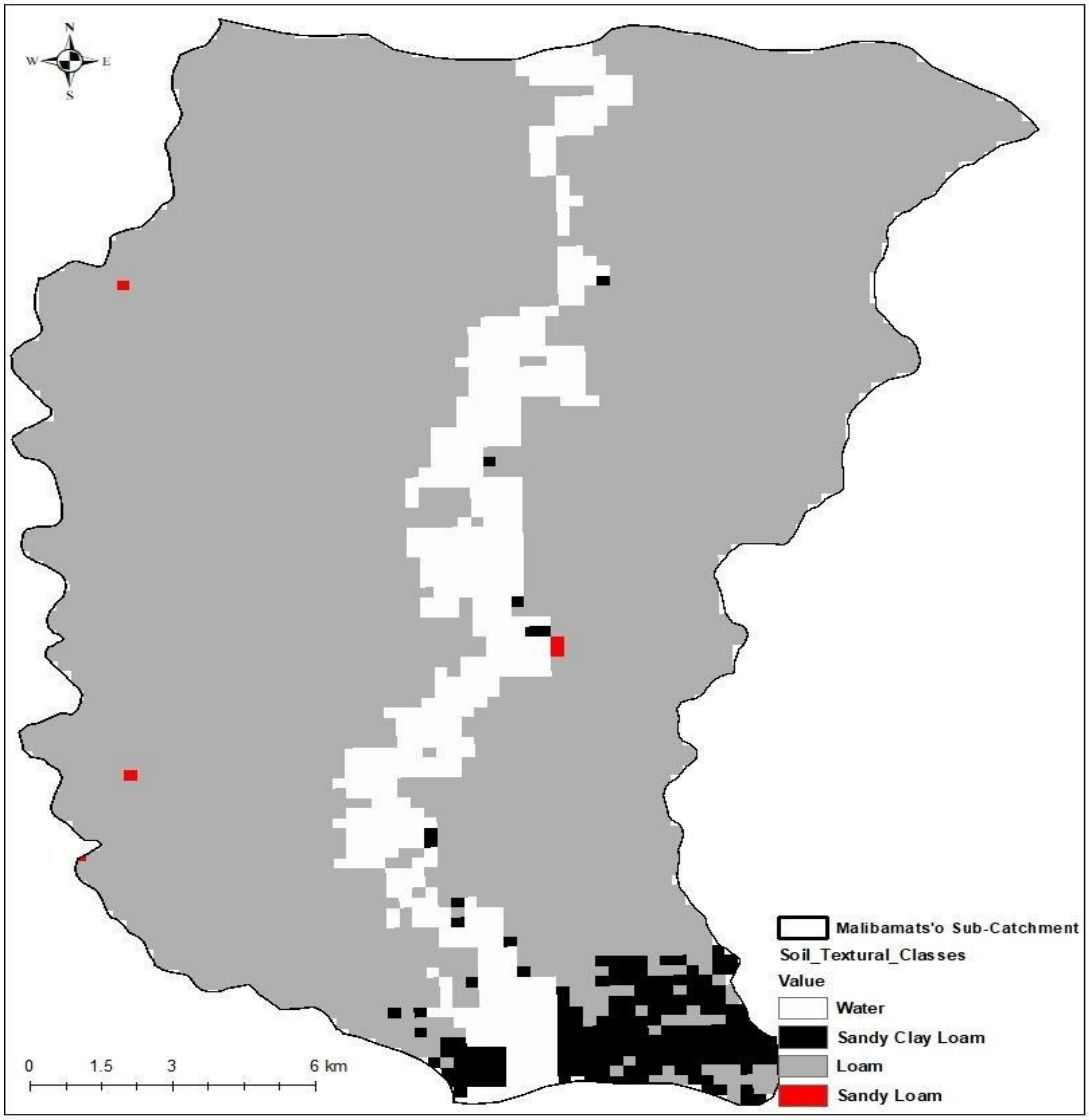

Figure 11: Soil Texture Map

Table 8: Frequency Ratio Value Calculations for Road Distance

Parameter	Classes	Class Pixels	% Class Pixels (a)	Landslide Pixels	% Landslide Pixels (b)	FR (b/a)
Road Distance (m)	0 - 50	11342	3.36	34	14.17	**4.22**
	50 - 100	10516	3.11	36	15.00	**4.82**
	100 - 200	19442	5.75	41	17.08	**2.97**
	200 - 400	38055	11.26	59	24.58	**2.18**
	400 - 1000	107864	31.92	65	27.08	0.85
	>1000	150709	44.60	5	2.08	0.05
Total		337928	100	240	100	**15.09**

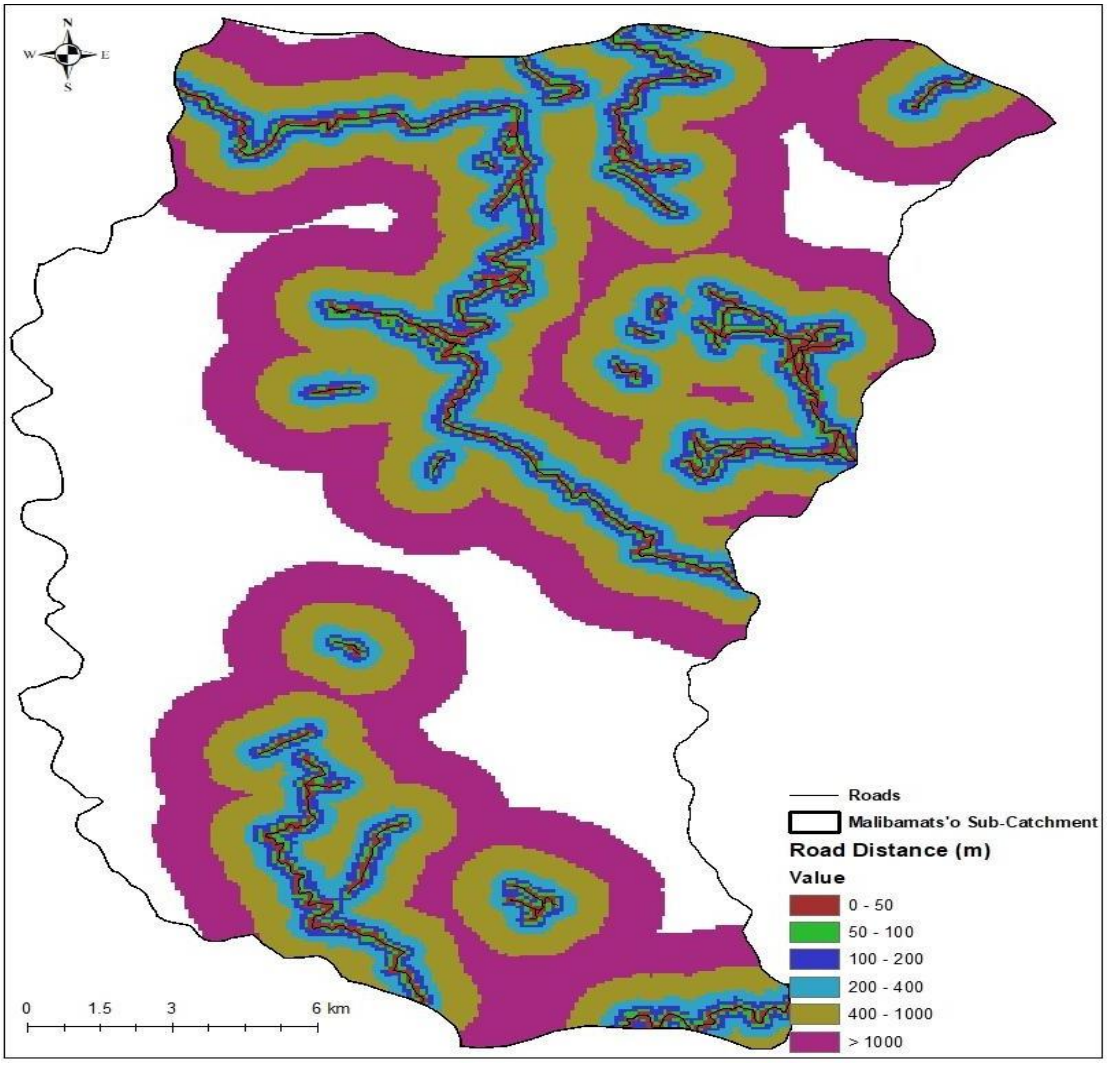

Figure 12: Distance to Roads Map

Table 9: Frequency Ratio Value Calculations for Stream Distance

Parameter	Classes	Class Pixels	% Class Pixels (a)	Landslide Pixels	% Landslide Pixels (b)	FR (b/a)
Stream Distance (m)	0 - 200	181408	35.22	50	20.83	0.59
	200 - 400	110393	21.43	20	8.33	0.39
	400 - 600	57620	11.19	0	0.00	0.00
	600 - 800	34886	6.77	12	5.00	0.74
	800 - 1000	25588	4.97	123	51.25	**10.32**
	>1000	105227	20.43	35	14.58	0.71
Total		515122	100	240	100	**12.75**

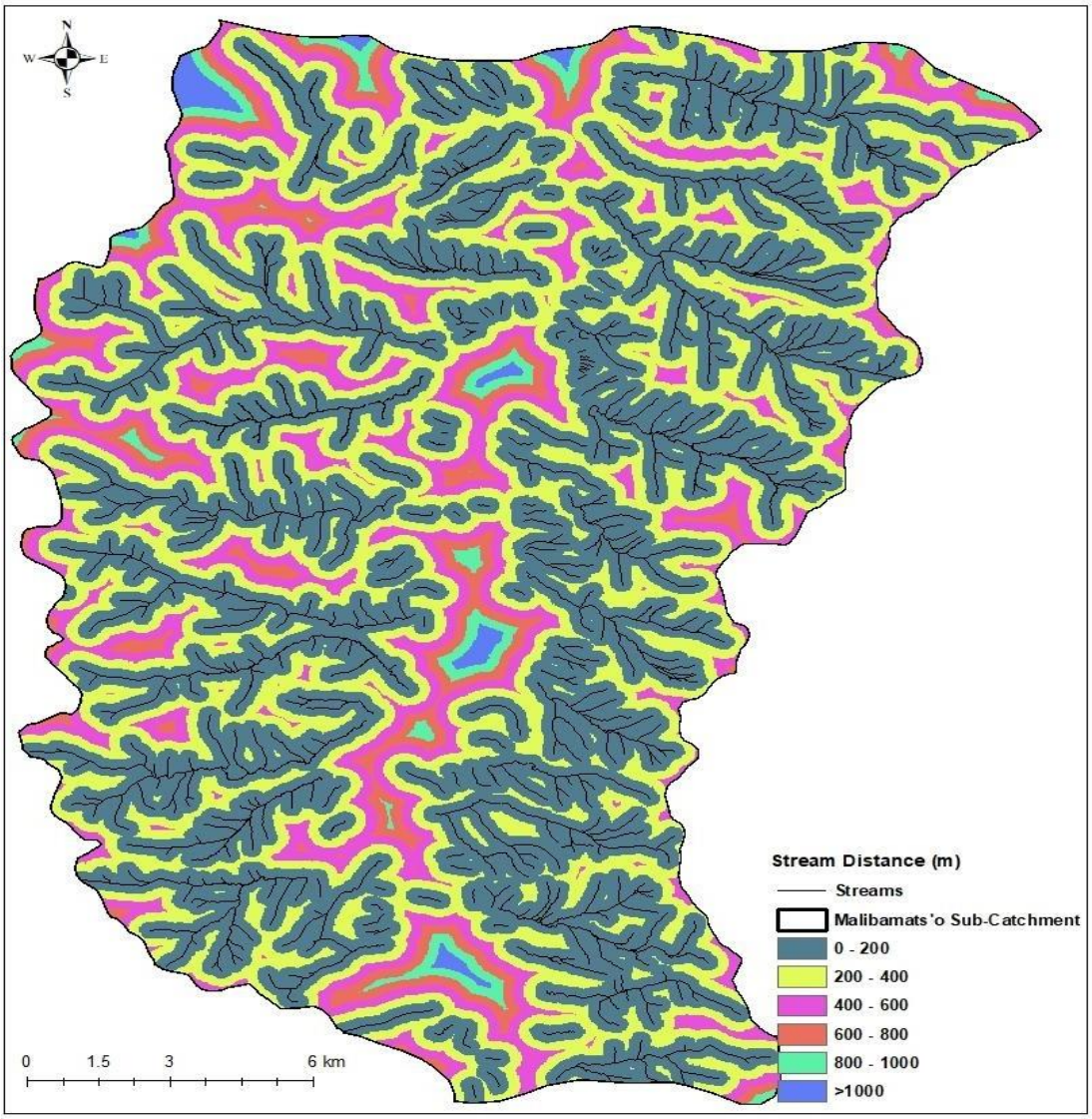

Figure 13: Distance to Streams Map

Table 10: Frequency Ratio Value Calculations for Rainfall Distribution

Parameter	Classes	Class Pixels	% Class Pixels (a)	Landslide Pixels	% Landslide Pixels (b)	FR (b/a)
Rainfall (mm)	577 - 615	67886	12.31	0	0.00	0.00
	615 - 653	158262	28.70	0	0.00	0.00
	653 - 691	107163	19.44	0	0.00	0.00
	691 - 729	110535	20.05	70	29.17	**1.45**
	729 - 767	107535	19.50	170	70.83	**3.63**
Total		551381	100	240	100	**5.09**

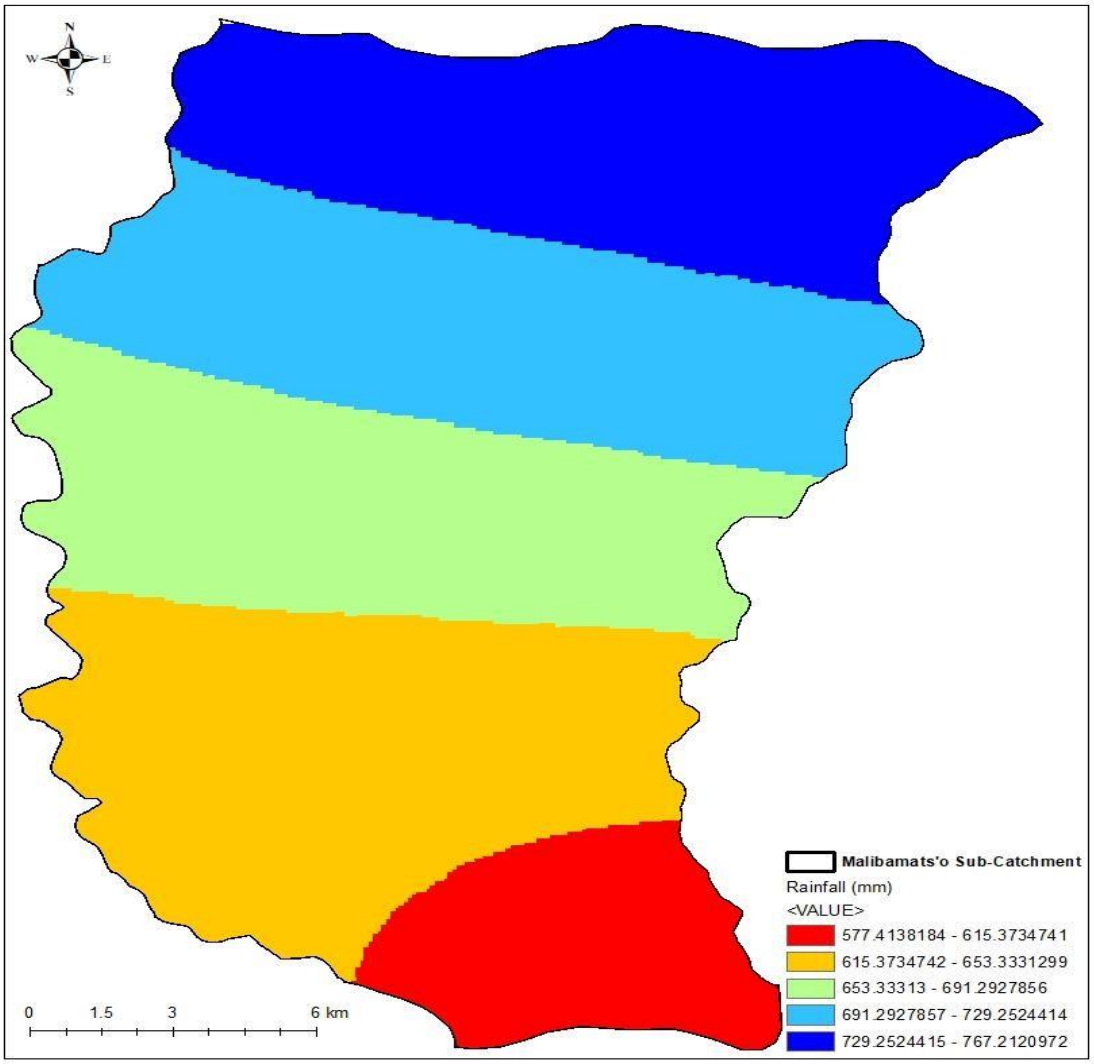

Figure 14: Rainfall Distribution Map

Table 11: Frequency Ratio Value Calculations for NDVI

Parameter	Classes	Class Pixels	% Class Pixels (a)	Landslide Pixels	% Landslide Pixels (b)	FR (b/a)
NDVI	-0.058 - 0.057 (Water Body)	24491	6.84	2	0.83	0.12
	0.057 - 0.172 (Bare Land)	95511	26.68	140	58.33	**2.19**
	0.172 - 0.287 (Sparse Vegetation)	223611	62.45	94	39.17	0.63
	0.287-0.402 (Moderate Vegetation	13712	3.83	4	1.67	0.44
	0.402 - 0.517 (Dense Vegetation)	722	0.20	0	0.00	0.00
Total		358047	100	240	100	**3.37**

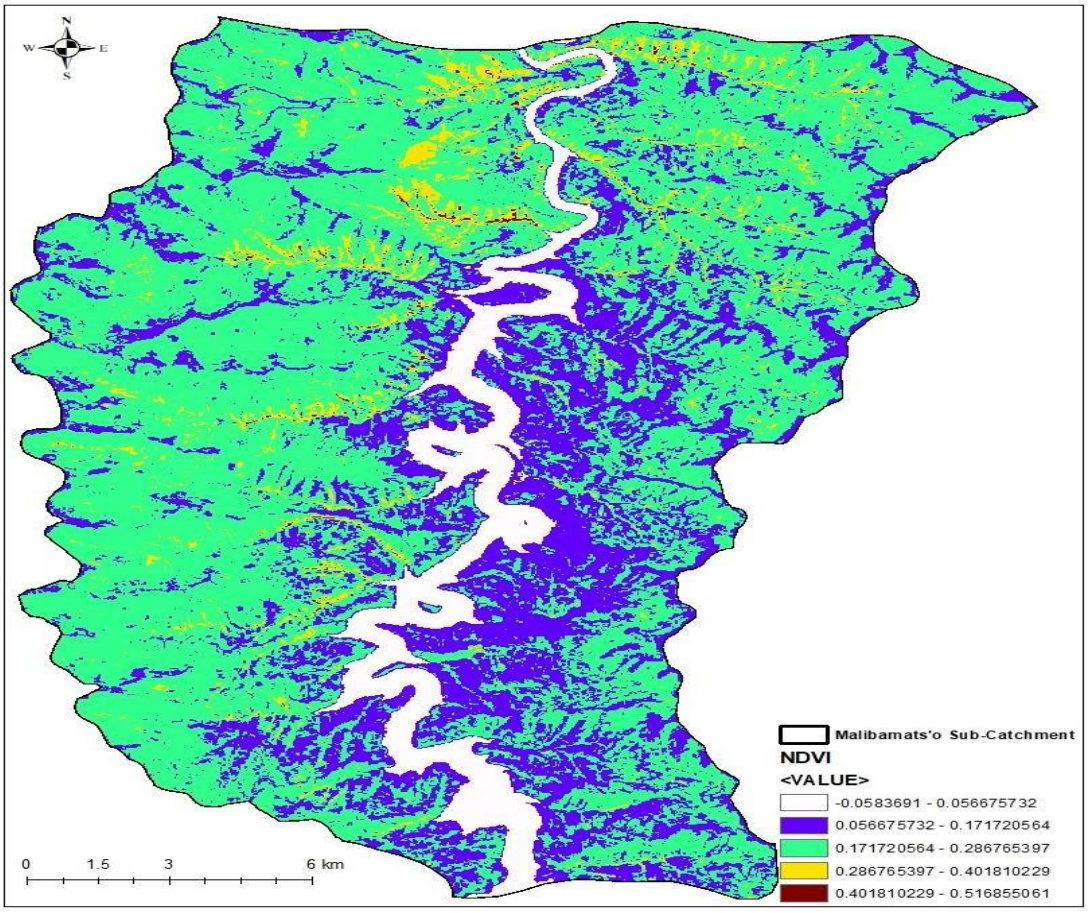

Figure 15: Normalized Difference Vegetation Index (NDVI) Map

4.1.1 Curvature

The flat curvature class occupies the greatest proportion of the catchment area (37.89%) and also accounts for the highest proportion of landslides (42.08%), resulting in a Frequency Ratio (FR) of 1.11. This shows a slightly positive interrelationship between flat terrain and occurrence of slope failure. The concave curvature class, which includes 28.64% of the area, experiences 32.92% of the landslides, with an FR of 1.15. This is the highest FR among the three curvature types, indicating a modest but more significant correlation between concave slopes and landslide events. In contrast, the convex curvature class covers 33.47% of the area but only contributes 25.00% of the landslides, giving it an FR of 0.75. This reflects a weaker correlation and suggests convex areas are less susceptible to landslides in this region.

Curvature plays a vital part in controlling water flow, sediment accumulation, and slope stability, key factors in landslide susceptibility. In this study, concave areas showed a higher frequency ratio (FR = 1.15), suggesting an increased likelihood of landslide occurrence. This agrees with the results of Kebeba et al. (2024) in the maze catchment, Omo valley, southern Ethiopia, where concave slopes were at greater risk to landslides because of their tendency to collect runoff, increasing pore pressure and weakening slope materials.

Similarly, Gulbet and Getahun, (2024) noted that concave topographies in Awabel Woreda, Ethiopia are often linked with higher landslide susceptibility, particularly when intersecting with steep slopes and weak lithological formations. These zones act as natural collectors of surface water, promoting subsurface saturation and potential slope failure.

Interestingly, flat areas in the present study showed a relatively high Frequency Ratio (FR) of 1.11, suggesting a positive correlation with landslide occurrence. Naturally, flat or gently sloped terrain is typically less susceptible due to minimal gravitational force, slower runoff, and higher soil cohesion. However, this pattern can shift with human activities like farming and infrastructure development, which disrupt drainage and weaken soil structure. The elevated risk observed may result from such anthropogenic pressures. This finding contrasts with many studies linking landslide susceptibility to steep slopes and specific terrain curvature, particularly convex and concave forms due to concentrated gravitational forces and water flow. In contrast, flat curvature is generally found to be less prone to failure (Addis, 2023; Kebeba et al., 2024).

Convex slopes, with a lower FR (0.75), appear more stable due to their role in dispersing water and limiting its infiltration into the soil. These results are in correspondence with those of (Moragues et al., 2024) in the Northern part of Los Glaciares National Park, Southern Patagonia, Argentina, where convex forms were associated with lower landslide density due to reduced saturation and erosion processes.

4.1.2 Slope Angle

The highest landslide frequency is observed on moderate slopes (11–22°) with a Frequency Ratio (FR) of 1.62, showing that this slope category is significantly more prone to slope failure than expected under random distribution. The second most affected slope class is the steep slope range (33–45°) with an FR of 1.25, which still shows some positive correlation with landslide occurrences. In contrast, gentle slopes (<11°) and very steep slopes (>45°) show FR values below 1, suggesting that landslide incidents are less frequent in those areas. These results indicate that moderate and certain steep slope angles are more susceptible to landslide activity in the Malibamatšo catchment area.

The observed high frequency of landslides on moderate slopes (11–22°) is consistent with findings from several studies across different geographies, which have identified mid-range slope gradients as particularly vulnerable (Javier and Kumar, 2019; Moragues et al., 2024). These slopes are often the most accessible for man-made activities such as agriculture, terracing, and road development. Agricultural practices and terracing disturb the natural soil structure, reducing its cohesion and slope stability over time. Similarly, road construction on these gradients alters the natural drainage patterns, increasing water infiltration and weakening the slope materials. The combination of these anthropogenic pressures significantly elevates landslide susceptibility on moderate slopes.

Sonker et al. (2022) found that landslide susceptibility was elevated in mid-slope ranges due to farming practices and infrastructural developments that weaken the slope materials. Vegetation removal, often for cultivation or settlements, reduces slope resistance. In the highlands of Ethiopia, Sisay et al. (2024) highlighted how vegetation clearance significantly increased susceptibility, as roots are crucial for soil cohesion on inclined surfaces.

While steep slopes (33–45°) do exhibit elevated susceptibility due to gravity-driven processes, very steep slopes (>45°) often have limited soil cover, making mass movement less likely simply due to the absence of loose materials. This observation matches findings by Sonker et

al., 2022 in the Sikkim Himalaya, where steep and rocky terrains were less affected by landslides than mid-slope ranges with deeper, disturbed soils.

4.1.3 Elevation

The elevation range of 2473–2684 meters is the most landslide-prone, with a high FR of 2.61, indicating a strong positive correlation despite covering only 23.18% of the area while accounting for 60.42% of landslides. In contrast, at the lowest elevation (2051–2262 m), which occupies the largest area (33.48%), shows a lower FR of 0.75, suggesting fewer landslides than expected. The 2262–2473 m range has the lowest susceptibility (FR = 0.11), while the 2684–2895 m zone shows moderate influence (FR = 0.93). The highest elevations (2895–3107 m) recorded no landslides, with an FR of 0.00, implying limited disturbance.

The interrelationship between elevation and landslide susceptibility in the study area reveals a clear trend: mid-elevation zones (2473–2684 m) are highly exposed to landslides, with higher FR values. This finding aligns with previous studies that associate mid-altitude terrain with increased landslide activity because of the combined influence of steep slopes, intense land use, and higher rainfall concentration due to orographic lift. For instance, Moragues et al. (2024) found that in the Northern part of Los Glaciares National Park, Southern Patagonia, Argentina, landslide-prone zones were predominantly situated in mid-altitude belts, where slope instability is aggravated by agricultural activities and poor land management. Similarly, Sonker et al. (2022) emphasized that landslide susceptibility is enhanced in Sikkim Himalaya's highlands at elevations with a mix of anthropogenic disturbance and weak geological substrates.

The moderate landslide frequency at higher elevations (2684–2895 m) could be linked to geomorphic resistance, such as exposed rock surfaces or sparse land use, as observed by Das et al. (2023) in Upper Tista Basin, India. In such environments, while steepness persists, limited infrastructure and dense forest or alpine vegetation often mitigate slope failure. A similar observation was made by Sonker et al. (2022) in Sikkim Himalaya, where high-elevation areas with intact vegetation and less human interference exhibited lower landslide susceptibility despite their topographic complexity.

Interestingly, the lowest elevation class (2051–2262 m) also displayed relatively fewer landslides. This can be attributed to gentler slopes, better drainage, and possibly more cohesive soils, which reduce the likelihood of slope failure. This pattern was also found in the Siwalik

Zone of Chatara-Barahakshetra Section, Nepal by Thapa and Bhandari (2019a), where low-lying terrain with flatter topography and better-managed vegetation cover showed reduced landslide incidence.

In contrast, the complete absence of landslides in the highest elevation range (2895–3107 m) might reflect a combination of stable bedrock, sparse or no human activity, and natural inaccessibility. These observations mirror those in Sikkim Himalaya, as reported by Sonker et al. (2022), where high-altitude zones remained largely stable due to limited exposure to destabilizing factors like deforestation, agriculture, or infrastructure development. Moragues et al. (2024) also noted a similar phenomenon in the Northern part of Los Glaciares National Park, Southern Patagonia, Argentina, high elevations dominated by hard rock and minimal land use showed negligible landslide activity, even when steep slopes were present.

4.1.4 Slope Aspect

The Northeast-facing slopes show the highest landslide susceptibility with a Frequency Ratio (FR) of 5.28, indicating a very strong correlation between this aspect and landslide occurrence. Though this zone occupies only 11.28% of the region, it contains 59.58% of all recorded landslides, making it the most critical aspect in terms of landslide risk. The East-facing slopes also show a notable correlation with an FR of 1.99, covering 8.15% of the area and contributing 16.25% of the landslides. The Flat to North-facing slopes have a near-neutral FR of 1.02, with their proportion of landslides (18.75%) almost matching their area coverage (18.30%).

All other slope aspects Southeast, South, Southwest, West, Northwest, and North—have low or no landslide occurrence. Particularly, West, Northwest, and North-facing slopes recorded zero landslides, each with an FR of 0.00, suggesting these directions are the least susceptible to landslides in the area of study.

The present study shows that north-northeast-facing slopes exhibit the highest landslide susceptibility, indicating that slope aspect is a significant controlling factor for slope instability in Malibamatšo Sub-Catchment. Comparing this with the Nyahode and Buzi sub-catchments study in Zimbabwe, north- and northeast-facing slopes there had the lowest relative frequency (RF = 1.32–1.35), while south- and south-east-facing slopes were more susceptible (Muchaka et al., 2022). This contrast highlights the influence of local conditions such as rainfall distribution, soil type, and land use patterns, which can alter the relationship between aspect and landslide risk.

Similarly, in the Hanang District study in Tanzania, northeast-facing slopes had a lower FR (0.0092) than south- and south-west-facing slopes, suggesting that south-facing slopes were generally more prone to failure under the prevailing climatic and topographic conditions (Muhimbula, 2025). However, in the present study area, north-northeast-facing slopes recorded the highest susceptibility, which may be related to regional rainfall patterns, soil properties, and geomorphology, leading to increased moisture accumulation and reduced slope stability in these aspects.

These comparisons underscore that slope aspect alone does not universally dictate landslide risk. Rather, its influence is context-specific and interacts with other conditioning factors such as lithology, slope angle, soil properties, and land use. The observed differences between studies in Zimbabwe, Tanzania, and the present site highlight the necessity of site-specific analysis when producing landslide susceptibility maps, particularly for hazard mitigation and infrastructure planning.

4.1.5 Land Use Land Cover

The land cover classes most associated with landslide occurrence are Agricultural Land and Bareland, with Frequency Ratios (FR) of 2.29 and 2.21, respectively. Although these classes occupy 14.92% and 18.27% of the area, they account for 34.17% and 40.42% of landslide incidents. This indicates a significant interrelationship between these land uses and landslides. Sparse vegetation (FR = 0.95) contributes nearly proportionally to its area coverage (18.77% of area, 17.92% of landslides), indicating a neutral or average relationship. Shrubland, grassland, and built-up areas show low FR values (0.33, 0.06, and 0.15 respectively), suggesting lower landslide susceptibility. Notably, water bodies account for 0% of landslides (FR = 0.00), indicating no contribution to slope failure.

Land Use/Land Cover (LULC) serves an important function in influencing landslide susceptibility, mainly through its effect on vegetation cover, infiltration, slope stability, and human disturbance (Abay et al., 2025; Sonker et al., 2022).

The results of this study indicate that agricultural land (FR = 2.29) and bareland (FR = 2.21) are the most vulnerable to slope failure in the catchment. This matches the findings by Sisay et al. (2024), and Sonker et al. (2022) who observed that agricultural practices such as ploughing, and terracing, deforestation disrupt slope integrity, reduce vegetation cover, and enhance surface runoff, key contributors to slope failure. Furthermore, bare land, characterized by

exposed and disturbed soils, lacks root reinforcement and protective canopy cover, making it highly vulnerable to erosion and mass movement, as emphasized by Alamrew et al., (2024) and Manopkawee and Mankhemthong, (2025).

Sparse vegetation and shrubland showed lower landslide occurrences. Although these land covers are somewhat degraded, their remaining vegetation still provides partial protection through root binding and moisture regulation, consistent with the observations by Alamrew et al. (2024) and Manopkawee and Mankhemthong (2025a).Built-up areas (FR = 0.15) recorded minimal landslide occurrences, which may be due to their location on relatively stable terrain or the presence of engineering controls, such as retaining walls. However, Built-up areas substitute natural vegetation with impermeable surfaces, resulting in increased surface runoff and decreased water infiltration(Ayele et al., 2025). This accelerates erosion on adjacent slopes (Sisay et al., 2024). Water bodies, as expected, show no landslide activity, as they represent low-lying or flat terrain where slope failure is highly unlikely.

4.1.6 Soil Texture

The Loam soil class dominates the study area, covering 86.64% of the total area and accounting for 100% of the recorded landslides. It has FR of 1.15, indicating a slightly higher-than-average susceptibility to landslides compared to its area coverage. Other soil types, including Sandy Clay Loam (3.34%), and Sandy Loam (0.09%), recorded no landslides (FR = 0.00), indicating no association with landslide occurrences in this region.

In contrast, soil texture exhibited minimal influence in this study. This finding differs from the results reported by Gulbet and Getahun, (2024a), who found that soil texture had a notable impact on landslide susceptibility in Awabel Woreda Ethiopian. The limited impact of soil texture in the current analysis may be due to the relatively uniform soil characteristics across the study area, which reduces spatial variability in geotechnical properties.

4.1.7 Rainfall

Landslide occurrences are highest near roads, especially in proximity ranges of 0 – 50m, 50m –100m, and 100m –200 m, with high FR of 4.22, 4.82, and 2.97 respectively. Though these classes represent small portions of the study area 3.36%, 3.11%, and 5.75%, they collectively account for 46.25% of all landslides, indicating strong susceptibility near roads. The class 200m – 400m also has an elevated FR of 2.18, showing a moderately high likelihood of landslide occurrences. In contrast, areas 400m – 1000m from roads have an FR of 0.85,

suggesting that there is no connection between this distance and landslide incidents, and the >1000m class, which occupies the greatest extent of the study area (44.60%), shows an FR of 0.05, indicating very low landslide occurrence in distant zones.

The Frequency Ratio values across the different stream distance classes indicate a weak or no significant influence of streams on landslide incidents in the study area. Contrary to common expectations, the highest FR value 10.32 is observed in the 800–1000 m buffer zone, which accounts for only 4.97% of the total area but contains 51.25% of all landslides. This unusually high concentration far from streams suggests no direct correlation between stream proximity and landslide events. The areas closer to streams, particularly the 0–200 m and 200–400 m classes have lower FR values of 0.59 and 0.39, despite collectively occupying over 56% of the total land area. Similarly, the 400–600 m buffer shows no landslide occurrences, with an FR of 0.00. Other distances such as 600–800 m and >1000 m have moderate FR values of 0.74 and 0.71 respectively, further supporting the idea that stream distance does not directly influence landslide susceptibility in this region.

The highest rainfall range, 729–767 mm exhibits the strongest influence on landslides, with the FR of 3.63. Although it covers only 19.5% of the study area, it accounts for 70.83% of all landslide occurrences. This strongly suggests that high rainfall levels are a major instigating factor for landslides in the catchment area. The 691–729 mm range also shows a moderate impact, with an FR of 1.45, accounting for 29.17% of landslides, despite covering 20.05% of the area. This confirms that moderate to high rainfall significantly increases landslide susceptibility. In contrast, the lower rainfall ranges, 577–615 mm, 615–653 mm, and 653–691 mm have zero landslide records and FR values of 0.00, even though they collectively span over 60% of the land area. This indicates that low rainfall zones are not prone to landslides.

Rainfall is broadly acknowledged as a primary natural instigator of landslides, particularly in mountainous and steep terrains. In the current study, a strong positive interrelationship between higher yearly rainfall and landslide incidents was discovered, with the highest Frequency Ratio (FR) of 3.63 recorded in the 729–767 mm rainfall zone. This finding underscores the significance of precipitation thresholds in initiating landslides.

This observation aligns with the study by (Ayele et al., 2025), which identified rainfall as a key factor increasing landslide risks in Gofa Zone, Southern Ethiopia. Their research, employing "Geospatial analysis of landslide susceptibility and safe relocation zones", demonstrated that areas with higher rainfall exhibited increased landslide susceptibility.

Similarly, Gulbet and Getahun, (2024a) conducted a landslide vulnerability analysis in Awabel Woreda, Ethiopia using the FR model and analytical hierarchy process method. Their study revealed that environmental variables, including rainfall, significantly contribute to landslide proneness. The assessment emphasized the role of rainfall in increasing pore pressure, contributing to slope failure.

In the Upper Tista Basin, India, Das et al. (2023) utilized a GIS-based data-driven bivariate statistical models for landslide susceptibility prediction. Their findings indicated that rainfall, among other factors, is a major contributing factor to landslides, particularly in regions with steep slopes and specific geological conditions. These studies collectively reinforce the significance of incorporating precipitation metrics within landslide assessment and risk management. The absence of landslide occurrences in the regions receiving less than 691 mm of annual precipitation in the current study suggests the existence of a minimum threshold below which slope failure is unlikely.

4.1.8 Land cover

NDVI classification reveals a strong relationship between vegetation cover and landslide susceptibility. The NDVI range of 0.057–0.172, which corresponds primarily to bare land, occupies 26.68% of the area but accounts for 58.33% of landslide incidences, leading to high frequency ratio (FR) of 2.19. This indicates that bare land areas are highly susceptible to landslides as a result of sparse vegetation cover and root systems that typically stabilize slopes. Sparse vegetation, represented by NDVI values between 0.172–0.287, covers the majority of the area (62.45%) but contributes only 39.17% of landslides, with a moderate FR of 0.63. This indicates a moderate level of susceptibility where some ground cover is present but not sufficient to prevent slope failure. Moderate vegetation (NDVI 0.287–0.402) shows a lower landslide impact (1.67%) and an FR of 0.44, suggesting increased slope stability as vegetation becomes denser. The NDVI class of 0.402–0.517, which represents dense vegetation, covers only 0.20% of the area and has no recorded landslides (FR = 0.00), indicating very low or negligible landslide susceptibility.

The highest landslide susceptibility (FR = 2.19) was observed in areas with Normalized Difference Vegetation Index (NDVI) values between 0.057 and 0.172, which correspond to regions with bare soil or sparse vegetation. Such vegetation conditions are typically associated with agricultural encroachment, overgrazing, or deforestation. This finding aligns with the results of Manopkawee and Mankhemthong (2025a), who noted that deforested and sparsely

vegetated areas are particularly prone to slope instability because of the limited root structures that enhance soil cohesion and reduce erosion. Similar results were observed by Fuad et al. (2024) in the Bandarban district, Bangladesh, where low NDVI values were strongly correlated with increased landslide activity.

As vegetation density increases (NDVI values in the range of 0.172 to 0.402), slope failure risk decreases, indicated by lower Frequency Ratio (FR) values. This trend reflects the stabilizing effect of moderate to dense vegetation, which improves slope integrity through root reinforcement, interception of rainfall, and reduction of surface runoff. Ayele et al. (2025) also highlighted the protective role of vegetation in their study in Gofa Zone, Southern Ethiopia, where areas with healthy plant cover exhibited lower landslide occurrences.

Interestingly, in areas with very dense vegetation (NDVI > 0.402), no landslide occurrences were recorded in the current study, reinforcing the conclusion that well-preserved vegetation cover provides a strong natural defense against slope failure. This pattern is consistent with findings by Kebeba et al. (2024), who emphasized that undisturbed vegetated regions tend to exhibit minimal landslide risk due to robust eco-hydrological stability.

4.1.9 Road Distance and streams

The analysis indicates that landslide susceptibility is significantly higher in areas within 50–100 meters of roads, with a Frequency Ratio (FR) of 4.82. This heightened risk is likely due to disturbances from road development practices including excavation, earth cutting along slopes, and vegetation removal, which can destabilize slopes and alter natural drainage patterns. The susceptibility decreases with increasing distance from roads, reaching minimal levels beyond 1 kilometer, where anthropogenic disturbances are reduced.

This pattern aligns with findings from Youssef et al. (2023), who reported elevated landslide risks along the Tizi N’tichka area on the national road (RN9) linking Marrakech and Ouarzazate area, attributing it to road-induced slope destabilization. Similarly, Kebeba et al. (2024) observed that proximity to roads significantly influences landslide occurrences in the maze catchment, omo valley, southern Ethiopia, due to construction related slope modifications. In Dejen District, Northwestern Ethiopia, (Addis, 2023) found that landslide frequency tends to rise as proximity to roads increases. Thus, both existing roads and ongoing construction activities appear to disrupt slope stability, thereby elevating the likelihood of landslide events, emphasizing the impact of road-induced disturbances.

In the present study, an unexpected pattern emerged where landslides predominantly occurred at greater distances from streams, particularly within the 800–1000 m range.

This pattern contrasts with typical findings in mountainous catchments, where proximity to streams is often correlated with increased likelihood of landslide risk linked to slope undercutting and soil saturation. For example, studies such as Kebeba et al. (2024) in the maze catchment, Omo valley, southern Ethiopia and Berhane et al. (2020b) in the Adwa-Adigrat mountain chains, northern Ethiopia found higher landslide frequencies closer to drainage networks. These studies highlight that landslides often initiate in proximity to streams due to the destabilizing influence of flowing water.

However, the current study reveals an inverse trend, landslides predominantly occur at greater distances from streams. This divergence may be explained by local factors. In contrast to studies where hydrological dynamics play a dominant role, our study area may be more influenced by anthropogenic disturbances and terrain characteristics. Similar findings are echoed by Manopkawee and Mankhemthong (2025a), who noted that while stream proximity is generally significant, its influence can be offset by land use and slope gradient, particularly in the Mae Chan River watershed, northern Thailand where variations in terrain slope extend far from drainage channels.

Further, in the Baso Liben district, Northwestern Ethiopia, Alamrew et al. (2024) observed that although proximity to streams is usually important, landslides can still occur at larger distances where deforestation and human activity have altered the landscape. This supports the hypothesis that in some contexts, geological and anthropogenic factors may overshadow the effects of hydrological proximity.

Therefore, the results of this study suggest that while stream proximity is a well-established factor in landslide susceptibility models, its role is not universal. Local land use patterns, slope morphology, and anthropogenic modifications can significantly modulate this relationship, leading to spatial patterns of landslide occurrence that deviate from expected norms.

4.1.10 Important Factors that Contribute to LSS

Based solely on the total frequency ratio (FR) values for each parameter, among all parameters, distance to roads stands out with the highest total FR, making it the most influential factor. This suggests a strong relationship between landslides and human-induced activities. Following this, slope aspect, land use/land cover (LULC), and rainfall show high total FR

values, placing them as the next most influential parameters. This reveals that, road distance, slope aspect, LULC and rainfall are the critical contributors of landslide in Malibamatšo.

These findings align closely with those of Sonker et al. (2022), who also identified distance to roads, NDVI, and land use/land cover (LULC) as the dominant factors influencing landslides in the Sikkim Himalaya region. This similarity reinforces the idea that anthropogenic disturbances are critical in regions undergoing development, especially in mountainous or rugged terrains.

When compared to other regions, the critical factors identified in Malibamatšo differ slightly, reflecting the site-specific nature of landslide conditioning factors. For instance, Moragues et al. (2024) in Argentina reported lithology, LULC, and geomorphology as the most influential variables. Similarly, Berhane et al. (2020) in Ethiopia emphasized the role of lithology, proximity to streams and lineaments, and slope angle. These factors are more reflective of natural geological and geomorphic controls in those regions.

In contrast, Manopkawee and Mankhemthong (2025) in the Mae Chan River watershed of northern Thailand also found that elevation, slope steepness, geology, and land cover were dominant. Notably, drainage proximity played only a minor role in their context similar to the current study where proximity to drainage did not emerge as a major contributing factor. This suggests that the degree to which each parameter influences landslides varies with environmental context, terrain characteristics, and human activity levels.

4.2 Landslide Susceptibility Mapping

The Landslide Susceptibility Index (LSI) was computed based on the equation:

$$LSI = \sum_{i=1}^{n} \mathrm{FR}i$$

This method integrates the influence of multiple conditioning parameters to assess landslide prone areas comprehensively. As per the index, zones with higher LSI values indicate greater susceptibility to landslides (Figure 16).

Following the calculation, the LSI, derived using weighted contributing factors, was employed to generate the Landslide Susceptibility Map (LSM), which classifies the study area into five distinct susceptibility zones: very low, low, moderate, high, and very high. (Figure 17).

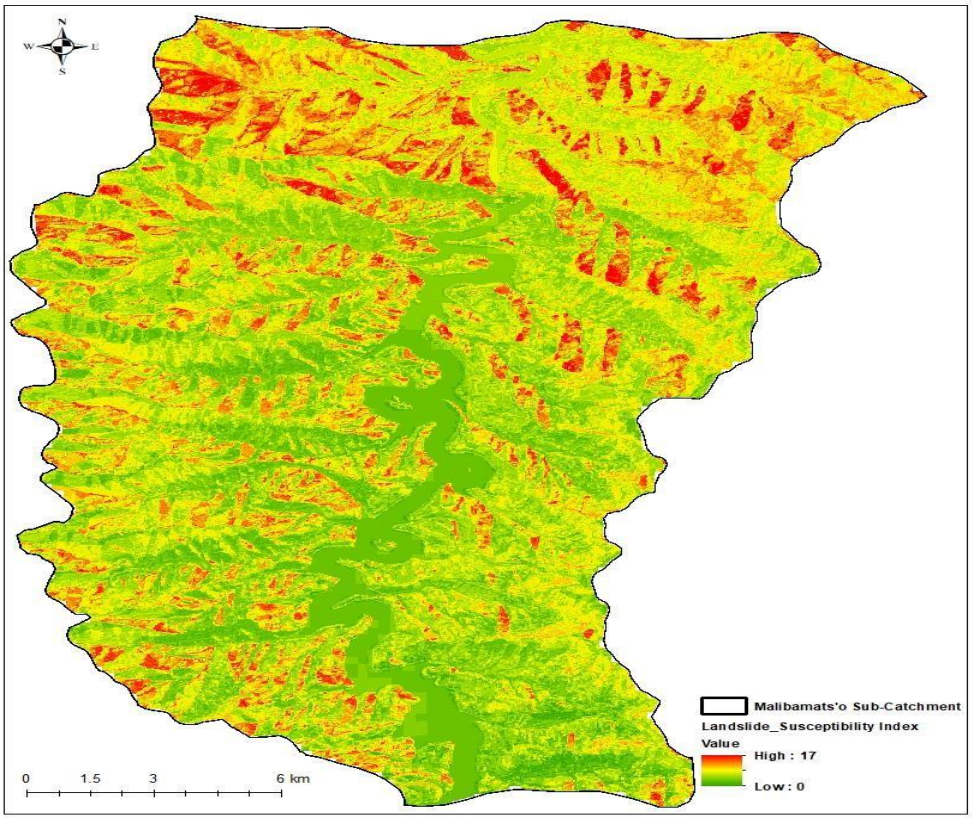

Figure 16: Final Weighted Map for Malibamatšo Catchment

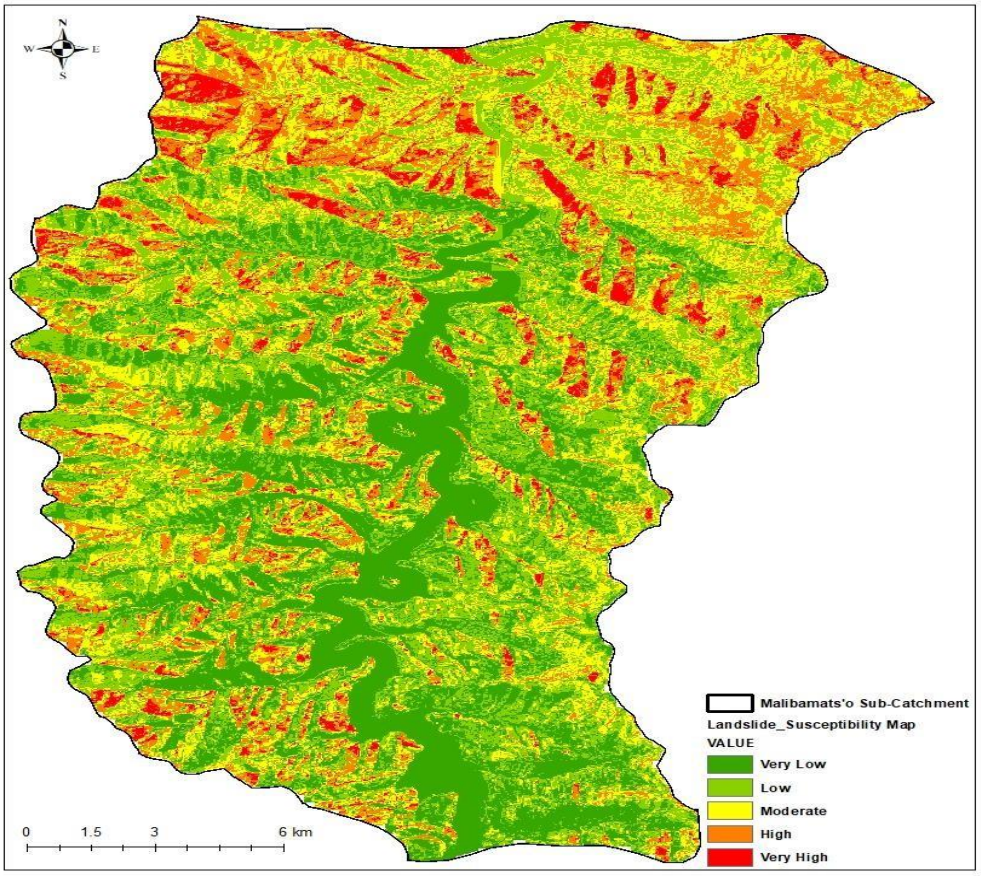

Figure 17: Landslide Susceptibility Map for Malibamatšo Catchment

According to the classification, approximately 91,565 pixels (25.89% of the area) fall within the very low susceptibility zone, 10,8617 pixels (30.71%) in the low susceptibility zone, 82,659 pixels (23.37%) in the moderate zone, 52,772 pixels (14.92%) in the high susceptibility zone, and 18,059 pixels (5.11%) in the very high susceptibility zone of the study area as shown in the Table 12.

Very Low to Low Susceptibility Zones cover 56.6 % (180.17 km2) of the study area (Table 12 and Figure 18). These zones are predominantly situated in the central part of the area of study, especially following the valley floors and lower elevation zones. They also appear more concentrated in the southern central region, suggesting more stable terrain with gentle slopes covered by dense vegetation and water bodies (Figure 17).

Moderate Susceptibility Zones cover 23.37% (74.39m2) of the study area (Table 12 and Figure 18). These are extensively spread across the study area but are specifically noticeable in the western, central-western, and eastern regions. These zones often act as transitional areas between the stable low-risk zones and more unstable high-risk zones. On the other hand, high to very high Susceptibility Zones cover 20% (63.74m2) of areas found along zones the northwestern, northern, northeastern, and southwestern parts of the study area. The spatial concentration of landslides in these areas aligns with conditions such as close proximity to roads, high rainfall intensity, northeast- and east-facing slopes, and the presence of agricultural fields.

Table 12: Landslide Susceptibility Rank and their Respective Area Coverage

Landslide Susceptibility Classes	**Area Pixels**	**Area (km^2)**	**Area in %**
Very Low	91565	82.41	25.89
Low	108617	97.76	30.71
Moderate	82659	74.39	23.37
High	52772	47.49	14.92
Very high	18059	16.25	5.11

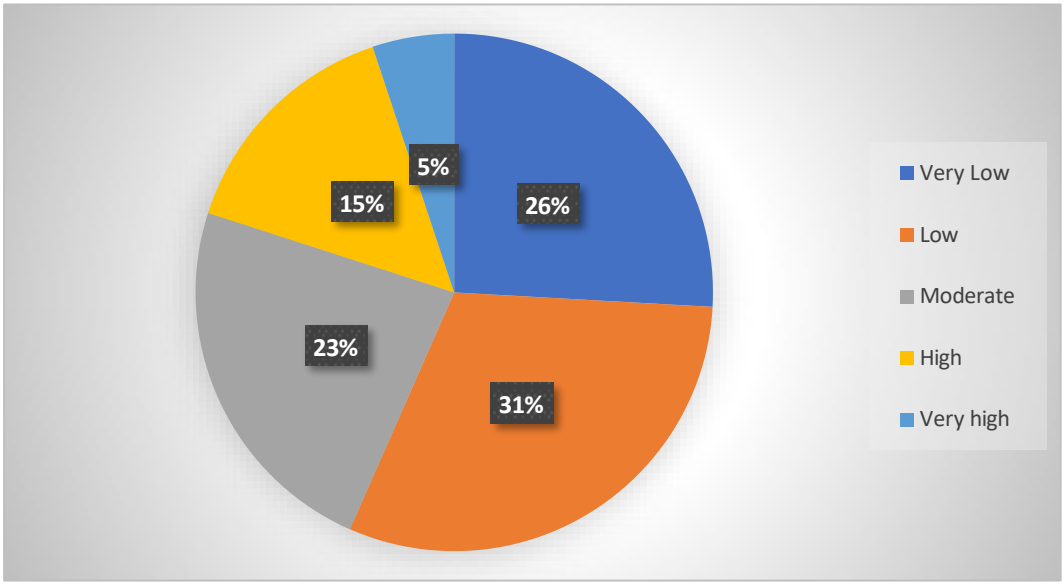

Figure 18: Percentage of the Area of the Landslide Susceptibility Classes

According to the results, the largest proportion of the study area, 31% falls under the Low susceptibility category, suggesting that these locations are relatively stable under current environmental and anthropogenic conditions. This is closely followed by Very Low susceptibility zones, which cover 26%, and Moderate susceptibility areas, which account for 23%, of the total area. These three classes combined make up approximately 80% of the study area, indicating that the greater part of the terrain is not presently at significant risk of landslides.

On the other hand, locations exhibiting High and Very High susceptibility represent 15% and 5% of the total study area, respectively. Although these areas form a smaller proportion of the landscape (combined 20%), they are of critical concern, as they are at greater risk of landslides especially in the course of the rainy season.

4.3 Validation

After generating the Landslide Susceptibility Map (LSM) utilizing Frequency Ratio (FR) model, validation is essential to ensure its reliability. Without validation, the LSM holds limited significance. In the current study, the reliability and effectiveness of the LSM were appraised with the help of the Area Under the Curve (AUC) derived from the success rate curve (Figure 19). The AUC value of the success rate curve was 0.89. An AUC value exceeding 0.8 signifies strong performance, indicating that the LSM generated with the help of Frequency Ratio model is accurate and reliable (Manopkawee and Mankhemthong, 2025).

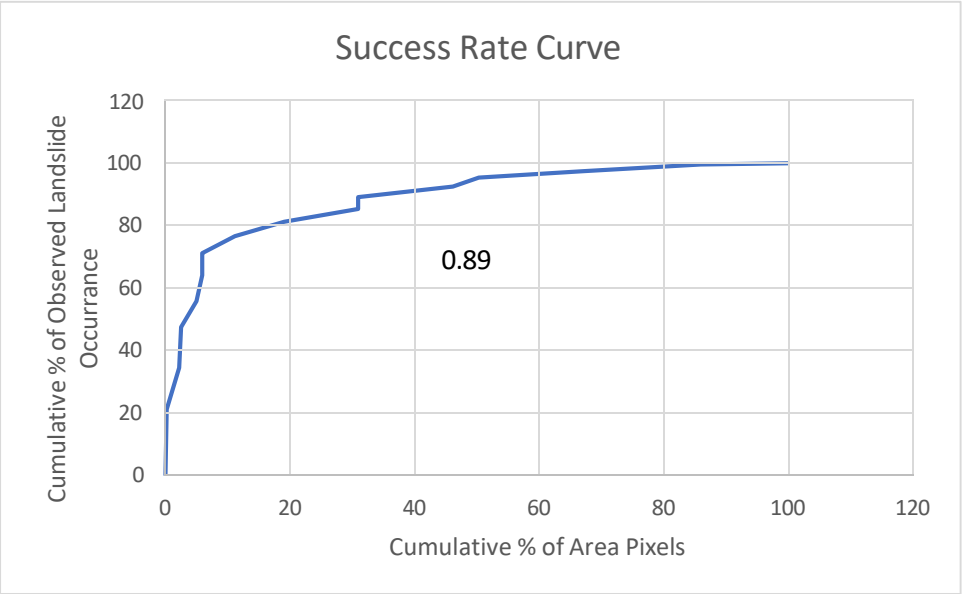

Figure 19: The Performance of the FR Model Using Success Rate Curve (SRC)

The success rate curve (SRC) shows a steep rise at the beginning, indicating that most known landslides lie within highly susceptible classes (Figure 19). This demonstrates the accuracy of the landslide susceptibility map. This curve shows how the distribution of susceptibility levels on the map aligns with the percentage of landslide pixels identified in landslide inventory (Binh Thai Pham et al., 2015).

Among the reviewed studies, the findings by Sonker et al. (2022) are the most comparable, with a reported success rate AUC of 87.3%, which also reflects a highly reliable model. Similarly, Moragues et al. (2024) reported an AUC of 0.804, suggesting good performance of the FR model in their analysis. Both studies reinforce the utility of the FR approach in producing dependable susceptibility maps across different geographic and geomorphologic contexts.

On the other hand, Pham et al. (2015) reported an AUC of 0.75, indicating a moderately good fit, while Thapa and Bhandari (2019) documented an AUC of 72.55%, showing a reasonable but comparatively less robust model outcome. The strong performance in the current study likely reflects the comprehensive inclusion of both environmental and human-induced factors, especially the significant role played by road proximity, slope aspect, LULC, and rainfall, which were recognized as key drivers to landslide occurrence in the catchment area.

4 Areas prone to landslides in the Malibamatšo catchment

Areas showing a high degree of susceptibility are principally situated in the northern and northeastern parts of the catchment (Figure 20). These zones tend to lie in close proximity to roads, on bare lands and agricultural lands, and on northeast- and east-facing slopes, which receive higher rainfall. Notably, several villages such as Ha Lejone, Ha Taunyane, Ha Sephapo, Ha Nkisi, Taung, Ha Poli, Liphofung and Ha Molatonyane, are located within or near these high-risk areas.

In contrast, the southern and southwestern parts of the catchment, around Maphutseng, Makoabating, Ha Mokhesi, Ha Kanono, Ha Chelane, and Ha Kosetabole are largely dominated by low to very low susceptibility classes. These regions are generally characterized by reduced road density, and less intense rainfall, contributing to the relatively lower landslide risk. The central portion of the map, stretching around Kobong, Ha Mallane, Ha Bereng, Ha Nts'eli and Ha Rafanyane, also displays moderate stability, with fewer red zones and more dominance of low and very low classes.

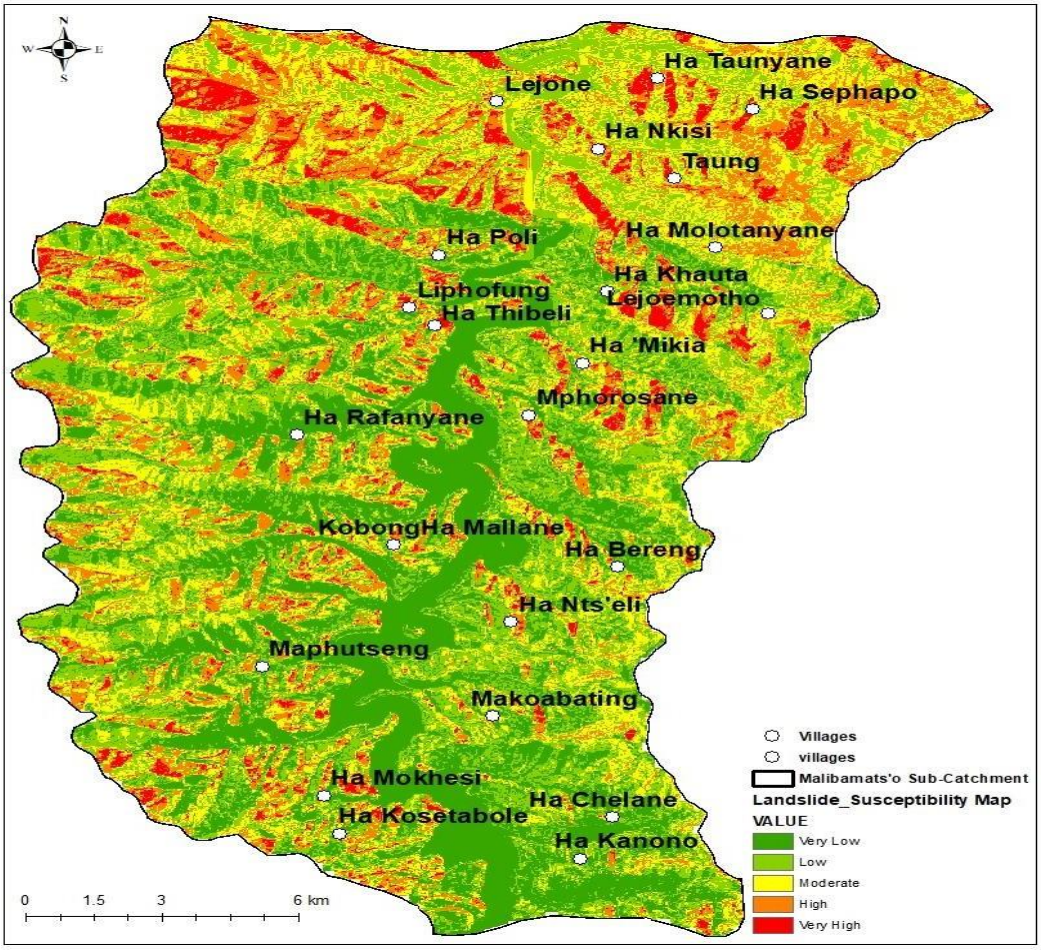

Figure 20: Landslide Susceptibility Map Showing Areas More Prone to Landslide

CHAPTER 5. CONCLUSION AND RECOMMENDATION

5.1 Conclusion

This study employed a GIS-based Frequency Ratio (FR) model to evaluate landslide risk potential in the study area, successfully identifying the key environmental and anthropogenic factors contributing to slope instability. The analysis revealed that slope failures occur most frequently in the vicinity of roads, on agricultural and bare lands, on northeast- and east-facing slopes, and in zones experiencing high rainfall intensity. These regions are critically at risk due to human disturbances and hydrological processes that increase soil saturation and weaken slope integrity.

Among the contributing factors, elevation, NDVI, slope angle, and curvature emerged as the second most influential in determining landslide susceptibility. Mid-elevation zones were especially at risk of landslides, possibly because of the combined effect of steeper slopes, land use concentration, and orographic rainfall effects. Areas showing low NDVI values, which suggest limited vegetation cover, were more susceptible possibly due to reduced root reinforcement. Moderate slopes (11–22°) were found to be highly vulnerable, likely due to agricultural activities and easier accessibility. Concave curvatures also showed higher landslide frequency, as they tend to accumulate water and sediment, increasing pore pressure.

These results highlight the complex interactions between topographic, climatic, and land-use variables in shaping landslide risk. The findings can inform land-use planning and hazard mitigation efforts by prioritizing monitoring and preventive measures in high-susceptibility zones, particularly those undergoing rapid land cover change or infrastructure development.

5.2 Recommendations

To promote sustainable land management, it is essential to prioritize slope stabilization along roads by installing retaining structures such as gabion walls, crib walls, and reinforced soil anchors, particularly on cut-slope sections adjacent to roadways. These measures help prevent landslides and erosion. Additionally, implementing systematic drainage systems, including properly placed outlets and culverts, is crucial for diverting surface runoff away from vulnerable embankments, thereby reducing water-induced slope failures. Conservation agriculture practices should also be adopted, particularly minimal tillage, to reduce soil disturbance, preserve soil structure, enhance water retention, and minimize erosion.

In areas affected by overgrazing, re-planting grasses is vital to restore vegetation cover and protect the soil from further degradation; using native or climate-adapted species ensures better resilience and survival. Furthermore, rotational grazing should be implemented to allow pastures time to recover, which maintains healthy vegetation, prevents overgrazing, and enhances both biodiversity and productivity. Agroforestry practices, which involve integrating trees and shrubs with crops and/or livestock, should also be promoted, as they improve soil fertility through organic matter inputs, provide shade and shelter, enhance biodiversity, and offer diversified income sources.

References

Abay, A., Mulugeta, A., Mebrahtu, G., 2025. GIS-based landslide susceptibility mapping using Frequency ratio method: A case study from Adigrat-Mugulat mountain chains, northern Ethiopia. Sci. Afr. 28, e02661. https://doi.org/10.1016/j.sciaf.2025.e02661

Adaawen, S., Motjotji, L., Schraven, B., Serraglio, D.A., 2023. Mainstreaming Migration, Environment and Climate Change into (Re)integration Initiatives in Lesotho. International Organization for Migration (IOM), Maseru, Lesotho.

Addis, A., 2023. GIS-Based Landslide Susceptibility Mapping Using Frequency Ratio and Shannon Entropy Models in Dejen District, Northwestern Ethiopia. J. Eng. 2023, 1–14. https://doi.org/10.1155/2023/1062388

Akintan, O.B., Olusola, J.A., Imole, O.P., Adeyemi, M.O., 2023. Geotechnical and GIS-based environmental factors and vulnerability studies of the Okemesi landslide, Nigeria. Reg. Sustain. 4, 249–260. https://doi.org/10.1016/j.regsus.2023.08.001

Alamrew, B.T., Kassawmar, T., Mengstie, L., Jothimani, M., 2024. Combined GIS, FR and AHP approaches to landslide susceptibility and risk zonation in the Baso Liben district, Northwestern Ethiopia. Quat. Sci. Adv. 16, 100250. https://doi.org/10.1016/j.qsa.2024.100250

Ali, Y., Gugsa, T.H., Raghuvanshi, T.K., 2024. GIS-based statistical analysis for landslide susceptibility evaluation and zonation mapping: A case from Blue Nile Gorge, Gohatsion-Dejen road corridor, Central Ethiopia. Environ. Chall. 16, 100968. https://doi.org/10.1016/j.envc.2024.100968

Arumugam, T., Kinattinkara, S., Velusamy, S., Shanmugamoorthy, M., Murugan, S., 2023. GIS based landslide susceptibility mapping and assessment using weighted overlay method in Wayanad: A part of Western Ghats, Kerala. Urban Clim. 49, 101508. https://doi.org/10.1016/j.uclim.2023.101508

Ayele, N.A., Engda, E.M., Terefe, T.T., Leta, E., Reda, T.M., Jothimani, M., 2025. Geospatial analysis of landslide susceptibility and safe relocation zones: Insights from recent disasters in Gofa Zone, Southern Ethiopia. Quat. Sci. Adv. 17, 100272. https://doi.org/10.1016/j.qsa.2025.100272

Berhane, G., Kebede, M., Alfarah, N., Hagos, E., Grum, B., Giday, A., Abera, T., 2020. Landslide susceptibility zonation mapping using GIS-based frequency ratio model with multi-class spatial data-sets in the Adwa-Adigrat mountain chains, northern Ethiopia. J. Afr. Earth Sci. 164, 103795. https://doi.org/10.1016/j.jafrearsci.2020.103795

Binh Thai Pham, Dieu Tien Bui, Prakash Indra, Dholakia M. B, Gujarat Technological University, 2015. Landslide Susceptibility Assessment at a Part of Uttarakhand Himalaya, India using GIS – based Statistical Approach of Frequency Ratio Method. Int. J. Eng. Res. V4. https://doi.org/10.17577/ijertv4is110285

Broeckx, J., Vanmaercke, M., Duchateau, R., Poesen, J., 2018. A data-based landslide susceptibility map of Africa. Earth-Sci. Rev. 185, 102–121. https://doi.org/10.1016/j.earscirev.2018.05.002

Bryant, M.M., Turner, J.S., 2019. From thermodynamics to creativity: McHarg's ecological planning theory and its implications for resilience planning and adaptive design. Socio-Ecol. Pract. Res. 1, 325–337. https://doi.org/10.1007/s42532-019-00027-1

Chen, L., Guo, H., Gong, P., Yang, Y., Zuo, Z., Gu, M., 2021. Landslide susceptibility assessment using weights-of-evidence model and cluster analysis along the highways in the Hubei section of the Three Gorges Reservoir Area. Comput. Geosci. 156, 104899. https://doi.org/10.1016/j.cageo.2021.104899

Chen, Z., Song, D., Juliev, M., Pourghasemi, H.R., 2021. Landslide susceptibility mapping using statistical bivariate models and their hybrid with normalized spatial-correlated scale index and weighted calibrated landslide potential model. Environ. Earth Sci. 80, 324. https://doi.org/10.1007/s12665-021-09603-9

Chowdhury, Md.S., 2023. A review on landslide susceptibility mapping research in Bangladesh. Heliyon 9, e17972. https://doi.org/10.1016/j.heliyon.2023.e17972

Cohen, W.J., 2019. The legacy of Design with Nature: from practice to education. Socio-Ecol. Pract. Res. 1, 339–345. https://doi.org/10.1007/s42532-019-00026-2

Dam, N.D., Amiri, M., Al-Ansari, N., Prakash, I., Le, H.V., Nguyen, H.B.T., Pham, B.T., 2022. Evaluation of Shannon Entropy and Weights of Evidence Models in Landslide Susceptibility Mapping for the Pithoragarh District of Uttarakhand State, India. Adv. Civ. Eng. 2022, 6645007. https://doi.org/10.1155/2022/6645007

Daniels, T., 2019. McHarg's theory and practice of regional ecological planning: retrospect and prospect. Socio-Ecological Practice Research, 1(2), pp.197–208. https://doi.org/10.1007/s42532-019-00024-4

Das, J., Saha, P., Mitra, R., Alam, A., Kamruzzaman, M., 2023. GIS-based data-driven bivariate statistical models for landslide susceptibility prediction in Upper Tista Basin, India. Heliyon 9, e16186. https://doi.org/10.1016/j.heliyon.2023.e16186

Diko, M.L., Banyini, S.C. and Monareng, B.F. (2014) "Landslide susceptibility on selected slopes in Dzanani, Limpopo Province, South Africa," Jàmbá: Journal of Disaster Risk Studies, 6(1), p. 7 pages. Available at: https://doi.org/10.4102/jamba.v6i1.101.

Fitchett, J.M. and Mackay, A.W. (2025) "Diatomite evidence for a small palaeo mountain lake at 3400 m asl, Lesotho, southern Africa," Journal of Quaternary Science, 40(3), pp. 445–458. Available at: https://doi.org/10.1002/jqs.3643.

Fuad, N., Meandad, J., Haque, A., Sultana, R., Anwar, S.B., 2024. Landslide vulnerability analysis using frequency ratio (FR) model: a study on Bandarban district, Bangladesh.

Government of Lesotho, 2011. National Disaster Risk Reduction Policy. Maseru: Disaster Management Authority.

Greyling, A.C. and Hedding, D.W. (2025) "Geomorphometric indices over the Drakensberg basalts: Implications for landscape evolution of the Great Escarpment," South African Journal of Geomatics, 14(2).

Gulbet, E., Getahun, B., 2024. Landslide susceptibility mapping using frequency ratio and analytical hierarchy process method in Awabel Woreda, Ethiopia. Quat. Sci. Adv. 16, 100246. https://doi.org/10.1016/j.qsa.2024.100246

Huang, F., Chen, J., Du, Z., Yao, C., Huang, J., Jiang, Q., Chang, Z., Li, S., 2020. Landslide Susceptibility Prediction Considering Regional Soil Erosion Based on Machine-Learning Models. ISPRS Int. J. Geo-Inf. 9, 377. https://doi.org/10.3390/ijgi9060377

Igwe, O., 2018. The characteristics and mechanisms of the recent catastrophic landslides in Africa under IPL and WCoE projects. Landslides 15, 2509–2519. https://doi.org/10.1007/s10346-018-1064-3

Javier, D.N., Kumar, L., 2019. FREQUENCY RATIO LANDSLIDE SUSCEPTIBILITY ESTIMATION IN A TROPICAL MOUNTAIN REGION. Int. Arch. Photogramm. Remote Sens. Spat. Inf. Sci. XLII-3/W8, 173–179. https://doi.org/10.5194/isprs-archives-XLII-3-W8-173-2019

Kebeba, O., Shano, L., Chemdesa, Y., Jothimani, M., 2024. Integration of geospatial analysis, frequency ratio, and analytical hierarchy process for landslide susceptibility assessment in the maze catchment, omo valley, southern Ethiopia. Quat. Sci. Adv. 15, 100203. https://doi.org/10.1016/j.qsa.2024.100203

Khumalo, T.F., 2021. Social issues related to climate change and food production (crops), in: The Impacts of Climate Change. Elsevier, pp. 291–311. https://doi.org/10.1016/B978-0-12-822373-4.00012-4

Kolane, N., 2022. Graves left exposed. [online] Available at:https://www.thereporter.co.ls/2022/03/24/graves-left-exposed [Accessed 7 September 2024]

Lesotho Highlands Development Authority (2017) Volume 4: Annexure J – River Ecosystems Specialist Report. Contract LHDA No.: 6014. Prepared by Nepid Consultants. Document Ref: P2W-6014-DFR-0005. 8 October.

Lesotho News Agency (LENA). 2023. Landslide exposes dead bodies. [online] Available at: https://www.lena.gov.ls/landslide-expose-dead-bodies [Accessed 7 September 2024].

Letsie, M.M., Grab, S.W., 2015. Assessment of Social Vulnerability to Natural Hazards in the Mountain Kingdom of Lesotho. Mt. Res. Dev. 35, 115–125. https://doi.org/10.1659/MRD-JOURNAL-D-14-00087.1

LMS, 2017. Lesotho's Nationally Determined, Contribution under the United Nations Framework Convention on Climate Change. Ministry of Energy and Meteorology, Lesotho.

M. Viana, C., Boavida-Portugal, I., Gomes, E., Rocha, J., 2023. Introductory Chapter: GIS and Spatial Analysis, in: Rocha, J., Gomes, E., Boavida-Portugal, I., M. Viana, C., Truong-Hong, L., Thu Phan, A. (Eds.), GIS and Spatial Analysis. IntechOpen. https://doi.org/10.5772/intechopen.111735

MacVicar, C.N., Loxton, R.F., Lambrechts, J.J.N., Le Roux, J., De Villiers, J.M., Verster, E., Merryweather, F.R., Van Rooyen, T.H. & Von Harmse, H.J., 1991. Soils of the Basalt of the

Drakensberg Formation in KwaZulu-Natal. In: Soil classification: A taxonomic system for South Africa. Pretoria: Department of Agricultural Development, pp. 95–105.

Makonyo, M., Zahor, Z., 2023. GIS-based analysis of landslides susceptibility mapping: a case study of Lushoto district, north-eastern Tanzania. Nat. Hazards 118, 1085–1115. https://doi.org/10.1007/s11069-023-06038-2

Makonyo, M. and Zahor, Z. (2023) "GIS-Based Analysis of Landslides Susceptibility Mapping: The Case Study of Lushoto District, North Eastern Tanzania." In Review. Available at: https://doi.org/10.21203/rs.3.rs-2330359/v1

Manopkawee, P., Mankhemthong, N., 2025. Landslide susceptibility assessment using the frequency ratio model in the Mae Chan River watershed, northern Thailand. Quat. Sci. Adv. 17, 100263. https://doi.org/10.1016/j.qsa.2024.100263

Maseru Metro News, 2021. Search for herdboy buried in landslide continues. [online] Available at: https://www.maserumetro.com/news/news/search-for-herdboy-buried-in-landslide-continues/#google_vignette [Accessed 7 September 2024].

Mathebula, B 2015. Assessment of the surface water quality of the main rivers feeding the Katse Dam Lesotho, MSc Dissertation, University of Pretoria, Pretoria, viewed yymmdd <http://hdl.handle.net/2263/53521>

Moragues, S., Lenzano, M.G., Jeanneret, P., Gil, V., Lannutti, E., 2024. Landslide susceptibility mapping in the Northern part of Los Glaciares National Park, Southern Patagonia, Argentina using remote sensing, GIS and frequency ratio model. Quat. Sci. Adv. 13, 100146. https://doi.org/10.1016/j.qsa.2023.100146

Muchaka, F.A. et al. (2022) "Landslide susceptibility modelling in Nyahode and Buzi sub-catchments of Zimbabwe," Water Practice and Technology, 17(7), pp. 1535–1552. Available at: https://doi.org/10.2166/wpt.2022.069.

Muhimbula, J., Sumari, N.S. and Balz, T. (2025) "Landslide Susceptibility Assessment Using AHP, Frequency Ratio, and LSI Models: Understanding Topographical Controls in Hanang District, Tanzania," GeoHazards, 6(3), p. 58. Available at: https://doi.org/10.3390/geohazards6030058.

Ntloko, B.R. et al. (2024) "Success in restoring native plant communities on kimberlite mining dumps in the Afro-alpine Drakensberg region of Lesotho," Ecology and Evolution, 14(3), p. e11022. Available at: https://doi.org/10.1002/ece3.11022.

Perera, E.N.C., Jayawardana, D.T., Jayasinghe, P., Bandara, R.M.S., Alahakoon, N., 2018. Direct impacts of landslides on socio-economic systems: a case study from Aranayake, Sri Lanka. Geoenvironmental Disasters 5, 11. https://doi.org/10.1186/s40677-018-0104-6

Pham, B.T., Bui, D.T., Indra, P. and Dholakia, M.B., 2015. Landslide susceptibility assessment at a part of Uttarakhand Himalaya, India using GIS–based statistical approach of frequency ratio method. International Journal of Engineering Research & Technology (IJERT), 4(11), pp.1–6.

Razavizadeh, S., Solaimani, K., Massironi, M., Kavian, A., 2017. Mapping landslide susceptibility with frequency ratio, statistical index, and weights of evidence models: a case

study in northern Iran. Environ. Earth Sci. 76, 499. https://doi.org/10.1007/s12665-017-6839-7

Reichenbach, P., Rossi, M., Malamud, B.D., Mihir, M., Guzzetti, F., 2018. A review of statistically-based landslide susceptibility models. Earth-Sci. Rev. 180, 60–91. https://doi.org/10.1016/j.earscirev.2018.03.001

Sebusi, M., 2022. Floods ravage Thaba Ntso even in death. Public Eye News, [online] 1 Nov. Available at: https://publiceyenews.com/2022/11/01/floods-ravage-thaba-ntso-even-in-death/ [Accessed 13 Oct. 2024].

Segue, W. S., Njilah, I. K., Fossi, D. H., & Nsangou, D. (2024). Advancements in mapping landslide susceptibility in Bafoussam and its surroundings area using multi-criteria decision analysis, statistical methods, and machine learning models. Journal of African Earth Sciences, 213. https://doi.org/10.1016/j.jafrearsci.2024.105237

Senanayake, S., Pradhan, B., Huete, A., Brennan, J., 2020. Assessing Soil Erosion Hazards Using Land-Use Change and Landslide Frequency Ratio Method: A Case Study of Sabaragamuwa Province, Sri Lanka. Remote Sens. 12, 1483. https://doi.org/10.3390/rs12091483

Sisay, T., Tesfaye, G., Jothimani, M., Reda, T.M., Tadese, A., 2024. Landslide susceptibility mapping using combined geospatial, FR and AHP models: a case study from Ethiopia's highlands. Discov. Sustain. 5, 474. https://doi.org/10.1007/s43621-024-00730-4

Skrzypczak, I., Kokoszka, W., Kogut, J., 2017. The Impact of Landslides on Local Infrastructure andthe Environment, in: Proccedings of 10th International Conference "Environmental Engineering." Presented at the Environmental Engineering, VGTU Technika, Vilnius Gediminas Technical University, Lithuania. https://doi.org/10.3846/enviro.2017.049

Sonker, I., Tripathi, J.N., Swarnim, 2022. Remote sensing and GIS-based landslide susceptibility mapping using frequency ratio method in Sikkim Himalaya. Quat. Sci. Adv. 8, 100067. https://doi.org/10.1016/j.qsa.2022.100067

Steiner, F., 2016. The application of ecological knowledge requires a pursuit of wisdom. Landsc. Urban Plan. 155, 108–110. https://doi.org/10.1016/j.landurbplan.2016.07.015

Tchuwa, I. and Makande, M. (2025) "Landslide susceptibility assessment using geotechnical characterization of collapsible and dispersive soils at Soche Hill, Blantyre, Malawi," Discover Geoscience, 3(1), p. 133. Available at: https://doi.org/10.1007/s44288-025-00232-4.

Tesfa, C., Sewnet, D., 2024. GIS-based MCDM approach for landslide hazard zonation mapping in east Gojjam zone, central Ethiopia. Quat. Sci. Adv. 15, 100210. https://doi.org/10.1016/j.qsa.2024.100210

Thapa, D., Bhandari, B.P., 2019. GIS-Based Frequency Ratio Method for Identification of Potential Landslide Susceptible Area in the Siwalik Zone of Chatara-Barahakshetra Section, Nepal. Open J. Geol. 09, 873–896. https://doi.org/10.4236/ojg.2019.912096

The Kingdom of Lesotho Report, 2015. Third United Nations Conference on Housing and Sustainable Urban Development (HABITAT III). Ministry of Local Government and Chieftainship Affairs.pdf

Thiery, Y. et al. (2024) “Landslide hazard assessment and mapping at national scale for Malawi,” Journal of African Earth Sciences, 212, p. 105187. Available at: https://doi.org/10.1016/j.jafrearsci.2024.105187

World Bank Group, 2021. Climate Risk Profile: Lesotho. Washington, D.C.: World Bank.

World Bank Group, 2023. National climate risk and vulnerability assessment (CRVA) for roads in Lesotho; development of vulnerability assessment tool for Lesotho roads and vulnerability assessments of selected catchment areas. [Online] Available at: https://www.preventionweb.net/publication/national-climate-risk-and-vulnerability-assessment-crva-roads-lesotho-development [Accessed 2 Sep 2024]

Youssef, B., Bouskri, I., Brahim, B., Kader, S., Brahim, I., Abdelkrim, B., Spalević, V., 2023. The contribution of the frequency ratio model and the prediction rate for the analysis of landslide risk in the Tizi N’tichka area on the national road (RN9) linking Marrakech and Ouarzazate. CATENA 232, 107464. https://doi.org/10.1016/j.catena.2023.107464

Zhang, G., Wang, S., Chen, Z., Liu, Y., Xu, Z., Zhao, R., 2023. Landslide susceptibility evaluation integrating weight of evidence model and InSAR results, west of Hubei Province, China. Egypt. J. Remote Sens. Space Sci. 26, 95–106. https://doi.org/10.1016/j.ejrs.2022.12.010